

1 When Case Reporting Becomes Untenable: Can Sewer 2 Networks Tell Us Where COVID-19 Transmission Occurs?

3 Yuke Wang^{1,*}, Pengbo Liu¹, Jamie VanTassell¹, Stephen P. Hilton¹, Lizheng Guo¹,
Orlando Sablon¹, Marlene Wolfe¹, Lorenzo Freeman², Wayne Rose², Carl Holt²,
Mikita Browning², Michael Bryan³, Lance Waller⁴, Peter F.M. Teunis¹, Christine L. Moe¹

4 September 29, 2022

¹Center for Global Safe Water, Sanitation, and Hygiene, Hubert Department of Global Health, Rollins School of Public Health, Emory University, Atlanta, Georgia 30322, USA.

²City of Atlanta Department of Watershed Management, Atlanta, Georgia 30303, USA.

³Georgia Department of Public Health, Atlanta, Georgia 30303, USA.

⁴Department of Biostatistics and Bioinformatics, Rollins School of Public Health, Emory University, Atlanta, Georgia 30322, USA.

*Address correspondence to Yuke Wang, Center for Global Safe Water, Sanitation, and Hygiene, Hubert Department of Global Health, Rollins School of Public Health, Emory University, 1518 Clifton Rd NE, CNR6040B, Atlanta, GA 30322. E-mail: yuke.wang@emory.edu

5 **Abstract**

6 *Word Limit: 150*

7 Monitoring SARS-CoV-2 in wastewater is a valuable approach to track COVID-19 transmission.
 8 Designing wastewater surveillance (WWS) with representative sampling sites and quantifiable
 9 results requires knowledge of the sewerage system and virus fate and transport. We developed
 10 a multi-level WWS system to track COVID-19 in Atlanta using an adaptive nested sampling
 11 strategy. From March 2021 to April 2022, 868 wastewater samples were collected from in-
 12 fluent lines to wastewater treatment facilities and upstream community manholes. Variations
 13 in SARS-CoV-2 concentrations in influent line samples preceded similar variations in numbers
 14 of reported COVID-19 cases in the corresponding catchment areas. Community sites under
 15 nested sampling represented mutually-exclusive catchment areas. Community sites with high
 16 SARS-CoV-2 detection rates in wastewater covered high COVID-19 incidence areas, and adap-
 17 tive sampling enabled identification and tracing of COVID-19 hotspots. This study demonstrates
 18 how a well-designed WWS provides actionable information including early warning of surges
 19 in cases and identification of disease hotspots.

20 **Keywords:** COVID-19; wastewater surveillance; sampling design; community level; hotspot; adaptive
 21 sampling; Atlanta

22 Introduction

23 Since the early stages of the COVID-19 pandemic, wastewater surveillance (WWS) has been recognized
 24 as a valuable tool that can complement traditional epidemiological surveillance, to monitor the spread of
 25 COVID-19 and indicate trends in infection at different levels [1, 2, 3, 4]. Ideally, traditional epidemiologi-
 26 cal surveillance through monitoring the number of people who tested positive for the SARS-CoV-2, would
 27 provide timely and accurate estimation of COVID-19 incidence. However, many factors like asymp-
 28 tomatic infections, non-specific symptoms, diagnostic test sensitivity, limited diagnostic test reagents and
 29 testing centers, inadequate data collection and overburdened reporting systems, and public health poli-
 30 cies and human behavior could contribute to under-ascertainment, under-reporting, and delayed reporting
 31 of COVID-19 using standard disease surveillance approaches [5, 6]. With detection of SARS-CoV-2
 32 RNA in wastewater [7, 8, 9] and in stools from COVID-19 patients [10, 11] during the early COVID-19
 33 pandemic, WWS, previously utilized to monitor enteric diseases [12, 13, 14, 15], was proposed as an in-
 34 clusive, non-intrusive, inexpensive, sensitive, and scalable strategy to guide public health response to the
 35 COVID-19 pandemic [16, 17]. By September 2022, federal and local governments, health departments,
 36 municipalities, and universities in at least 70 countries had utilized WWS to monitor COVID-19 [18].
 37 The results of WWS have been used to alert local jurisdictions, guide resource allocation, enable targeted
 38 communications, and forecast clinical resource needs [3].

39 Most WWS studies have monitored and estimated the COVID-19 incidence at the city level [1, 19, 20] by
 40 collecting repeated grab or composite wastewater samples from downstream sites (e.g., inlets of wastewa-
 41 ter treatment facilities), that serve a large population. When COVID-19 is spreading, wastewater samples
 42 from downstream sites consistently contain detectable levels of SARS-CoV-2 RNA. To monitor temporal
 43 trends of COVID-19 incidence in the catchment population, quantification of SARS-CoV-2 RNA con-
 44 centration in wastewater is required. WWS has also been widely used at the institution level to monitor
 45 disease transmission and provide early warning of surges in cases or outbreaks [4, 21, 22, 23]. Usually,
 46 WWS for early warning is considered when the incidence is low. Frequent sampling is necessary to en-
 47 able a quick confirmation of an outbreak and a timely response. And the catchments of sampling sites
 48 would preferably be small, which enables targeted control measures. However, few WWS studies have
 49 focused on sampling upstream sites at the community/neighborhood level [24, 25]. Sampling upstream
 50 has the potential to identify disease hotspots within a larger area, which enables monitoring localized
 51 disease transmission and targeted public health interventions [25, 26]. Unlike sampling at wastewater

52 treatment facilities, sample collection at community sites across the sewer network is more complicated
 53 and requires more strategic sampling design in order to optimize the value of information and guide
 54 interpretation of the results [15, 27, 28, 29, 30, 31].
 55 In this study, we conducted COVID-19 WWS at the city and community level in the city of Atlanta. The
 56 objectives were to: (1) strategically design the WWS sampling by describing the sewer network in the
 57 city of Atlanta from a disease monitoring perspective, and developing and applying an algorithm to select
 58 and adapt community sampling sites across sewer networks; (2) examine the association between WWS
 59 results and COVID-19 incidence at different levels; and (3) illustrate the capacity of WWS to detect
 60 and monitor spatial COVID-19 hotspots at the community level. The knowledge gained in this study
 61 demonstrates the value of strategic sampling design for WWS to provide actionable information to guide
 62 public health response to COVID-19.

63 Results

64 *Atlanta Sewer Network*

65 We examined the network statistics (indegree and outdegree) and network topology of the Atlanta sew-
 66 erage system. The indegree and outdegree of a manhole in the sewer network are the numbers of sewer
 67 pipes going into and going out of the manhole, respectively. The city of Atlanta sewer network has a
 68 total of 52,787 sewer segments and 51,155 manholes. After excluding nodes with zero indegree or zero
 69 outdegree, the average indegree and outdegree were 1.40 and 1.04 respectively indicating it was mainly
 70 a tree topology network with some net topology structures. However, the sewer network topology varied
 71 in different areas. In newly developed areas with low population density, the sewer network includes
 72 more line topology components. In densely populated inner city areas with older sewerage structures,
 73 there are more cross-connections and greater connectivity. Figure 1 illustrates two sub-networks in our
 74 study: one near the center of the city (upstream of manhole 23370330601) and the other located more
 75 remotely (upstream of manhole 23330211001). The average indegree and outdegree were larger for the
 76 sewer network in the city center, which displays a more connected structure. Figures 2a and 2b show
 77 the spatial distribution of in- and outdegree in the Atlanta sewer network. The nodes with large indegree
 78 and outdegree are located mainly at the center of the city where the sewers are mainly combined sewers
 79 (Figure 2c).

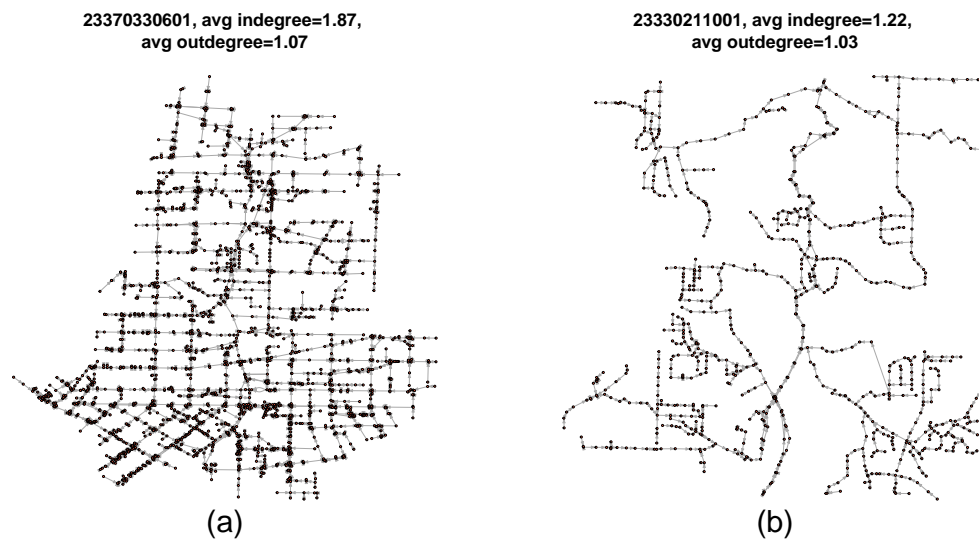


Figure 1: Two sewer sub-networks (a) within the center of the city and (b) in the periphery of the city.

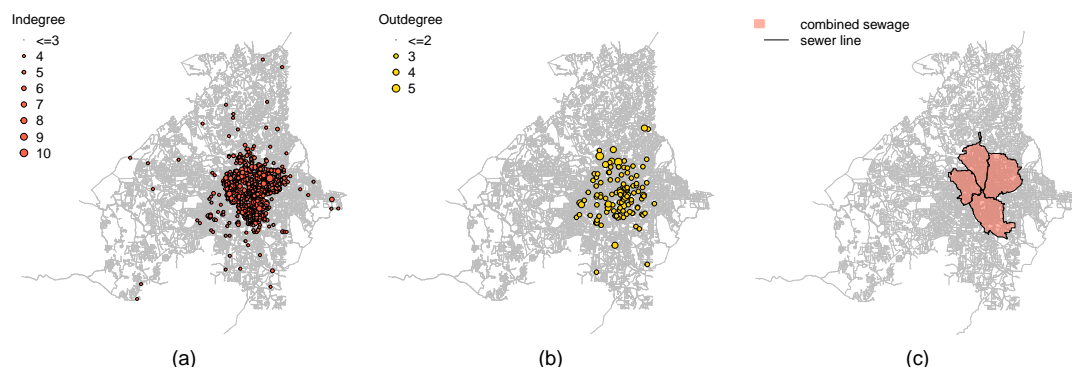


Figure 2: (a) Geographical distribution of manholes with large indegree on the sewer network; (b) Geographical distribution of manholes with large outdegree on the sewer network; (c) Areas with combined sewers in the city of Atlanta.

Influent Line Wastewater Surveillance Results

A total of 362 samples were collected from nine influent lines entering three wastewater treatment facilities during March 20, 2021–April 11, 2022 (Figure 3a). Figure 4 shows the concentrations of SARS-CoV-2 RNA in the wastewater samples from influent lines increased between July and August 2021, matching the temporal trend of reported cases in Fulton County, Georgia. When the reported cases decreased in October and November 2021, the SARS-CoV-2 RNA concentrations in wastewater stayed relatively high. In

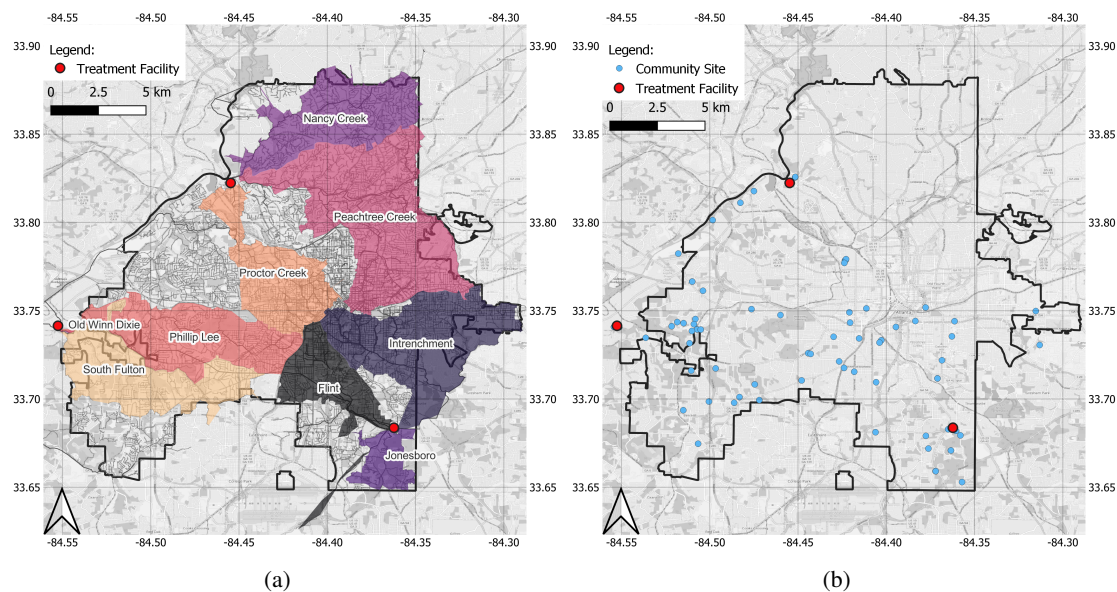


Figure 3: (a) Estimated catchment areas of nine influent lines sites in the city of Atlanta; The catchment area of Old Winn Dixie, which is very small, may not be visible. (b) locations for community sampling sites and school sampling sites.

late December, the SARS-CoV-2 RNA concentration in wastewater and the reported case numbers surged rapidly and then decreased in January 2022.

Correlation analysis showed that the concentration of SARS-CoV-2 RNA in wastewater and the number of daily reported COVID-19 cases in Fulton County were moderately correlated (Spearman ρ between 0.48–0.65) except for the South Fulton site (Spearman $\rho=0.33$). We also found strong correlations (Pearson's r between 0.70–0.98 and Spearman ρ between 0.67–0.95) between the SARS-CoV-2 RNA concentrations in the wastewater samples from those six influent line sites sampled for the entire study period (Supplementary Figure 2). For most influent line sites, the correlations between the concentrations of SARS-CoV-2 RNA in wastewater and the reported cases (in Fulton County or in the catchment area) 7–12 days later were higher than the correlation between the concentrations of SARS-CoV-2 RNA in wastewater and the reported cases at the day of wastewater sampling (Supplementary Figures 3 and 4).

Community Site Wastewater Surveillance Results

Figure 5 shows the overall WWS results from community sampling sites. A total of 506 Moore swab samples were collected from 56 manholes (Figure 3b). In the pilot phase 1 (April–May 2021), we col-

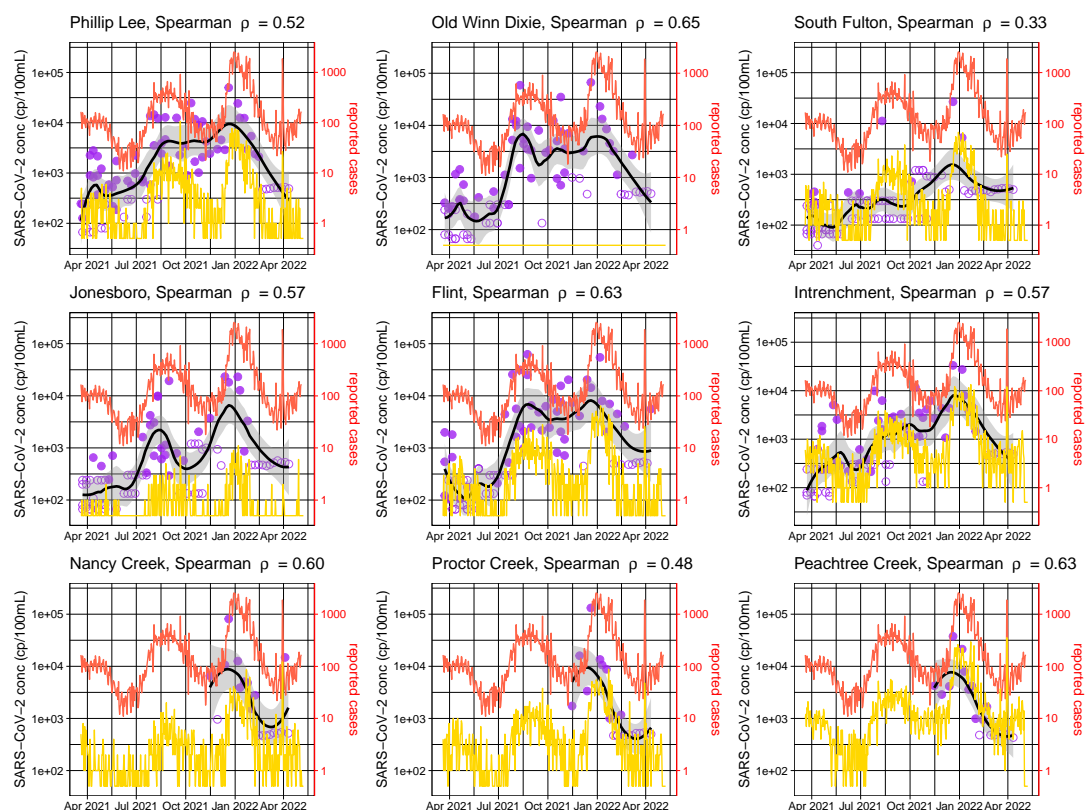


Figure 4: Temporal trends of the concentrations of SARS-CoV-2 RNA in wastewater from nine influent line sites and the reported case numbers during March 20, 2021–May 8, 2022. Solid purple symbols represent positive samples and open purple symbols show negative samples at the detection limit. The black line is the LOESS line for concentration of SARS-CoV-2 RNA, and the gray band represent the 95% confidence interval. The red line is the number of reported cases in Fulton County, Georgia. The yellow line is the number of reported cases in the catchment area of the influent site. Throughout the study period, no case was reported in the very small catchment area of Old Winn Dixie. The graph caption shows the Spearman correlation between the smoothed concentrations of SARS-CoV-2 RNA in wastewater and the number of reported cases in Fulton County.

100 lected wastewater samples from 20 community sites, each for a time period of two weeks. We detected
 101 samples positive for SARS-CoV-2 RNA at 7 sites, while the other 13 sites only produced weak positive
 102 or negative samples. The detection rates for SARS-CoV-2 RNA at community sites varied even between
 103 manholes in close proximity. In phase 2 with the targeted sampling (June–August 2021), the frequency
 104 of SARS-CoV-2 detection in the wastewater samples from community sites increased in July–September
 105 2021 along with a surge in number of reported COVID-19 cases in Fulton County. In phase 3 with the

106 nested sampling (September 2021–April 2022), samples from some community sites consistently had de-
 107 tectable SARS-CoV-2 RNA throughout the study period while other sites were only positive in December
 108 2021, when the numbers of reported cases surged to an unprecedented high level. Four community sites
 109 (Ruby Harper Blvd, Southside Industrial Parkway, Village Dr, and Walmart), which had low percentages
 110 of positive wastewater samples, were relocated at the end of December 2021 to four new sites, which

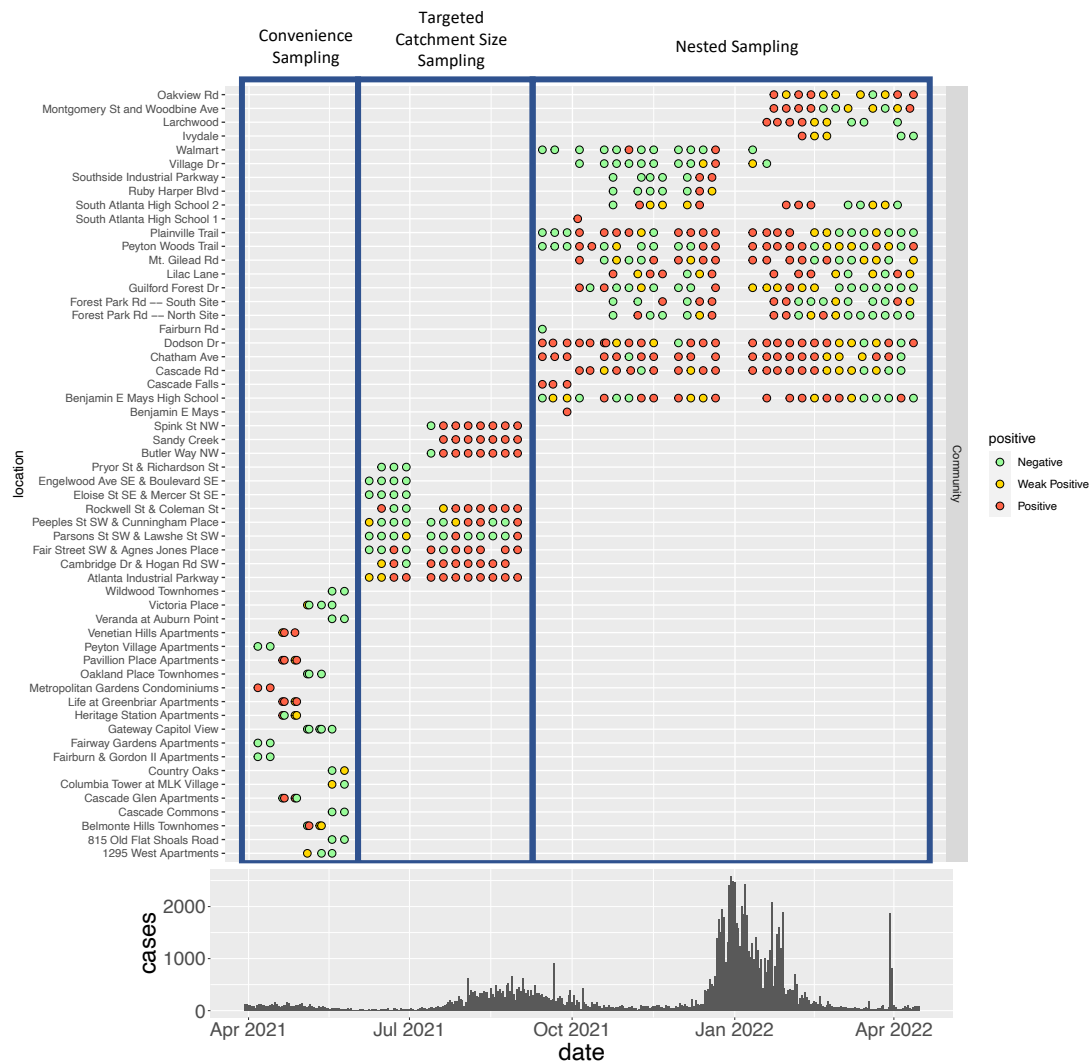


Figure 5: SARS-CoV-2 wastewater surveillance results for community sites and reported case numbers in Fulton County between March 20, 2021–April 15, 2022. The high reported case numbers in April 2022 were caused by a data dump (i.e., delayed reporting), and did not represent a surge in cases during that month.

111 had more positive samples compared to those sites that were dropped. In March–April 2022, when the
 112 incidence decreased to a relatively low level, some community sites were still positive for SARS-CoV-2
 113 RNA while their corresponding downstream influent line samples were negative (Figure 6, Supplemen-
 114 tary Figures 5, 6, and 7).
 115 With the nested sampling design in phase 3, we observed spatial agreement between SARS-CoV-2 RNA
 116 detection in wastewater from a community site and the number of cases reported within the catchment
 117 area of the same site. Figure 6 shows WWS results and cases reported side by side for the Phillip Lee
 118 sampling cluster (one downstream influent line site with multiple upstream community sites) as an ex-
 119 ample. Catchment areas of community sites with high SARS-CoV-2 detection rates in the wastewater
 120 (i.e., Chatham Ave and Plainville Trail) overlapped with areas with high numbers of reported COVID-19
 121 cases. In contrast, samples from the Walmart site, which has a relatively large catchment area, were only
 122 positive for SARS-CoV-2 RNA twice out of 13 samples. In this area, few cases were reported during the
 123 surveillance period. The results from other sampling clusters are included in the Supplementary Figures
 124 5, 6, and 7.

125 Discussion

126 As new variants emerge, SARS-CoV-2 continues to cause waves of infection across the globe [32]. After
 127 more than two years of COVID-19 pandemic, adherence to COVID-19 rules and guidance has declined
 128 [33, 34], and there are signs of fatigue in performing PCR tests for individual nasal swabs and report-
 129 ing daily confirmed COVID-19 case numbers accumulated among patients, caregivers, laboratories, and
 130 health departments. Such pandemic fatigue contributes to increasing and more heterogeneous underes-
 131 timation of COVID-19 incidence all over the world. Meanwhile, it is unrealistic to sustain large scale
 132 epidemiological surveillance systems based on individual diagnostic testing given the economic burden
 133 especially in countries where the resources are limited. WWS, as an inexpensive, sensitive, and non-
 134 intrusive method, could provide information about COVID-19 incidence at different geographic levels
 135 and is especially useful for populations where COVID-19 is under-ascertained and/or under-reported due
 136 to limited access to diagnostic testing or health behavior. With careful sampling designs, WWS can
 137 be utilized to examine temporal trends of COVID-19 incidence at the city level and to identify spatial
 138 COVID-19 hotspots at the community level. Such information differentiated by geographic level can
 139 directly inform and guide public health responses to COVID-19.

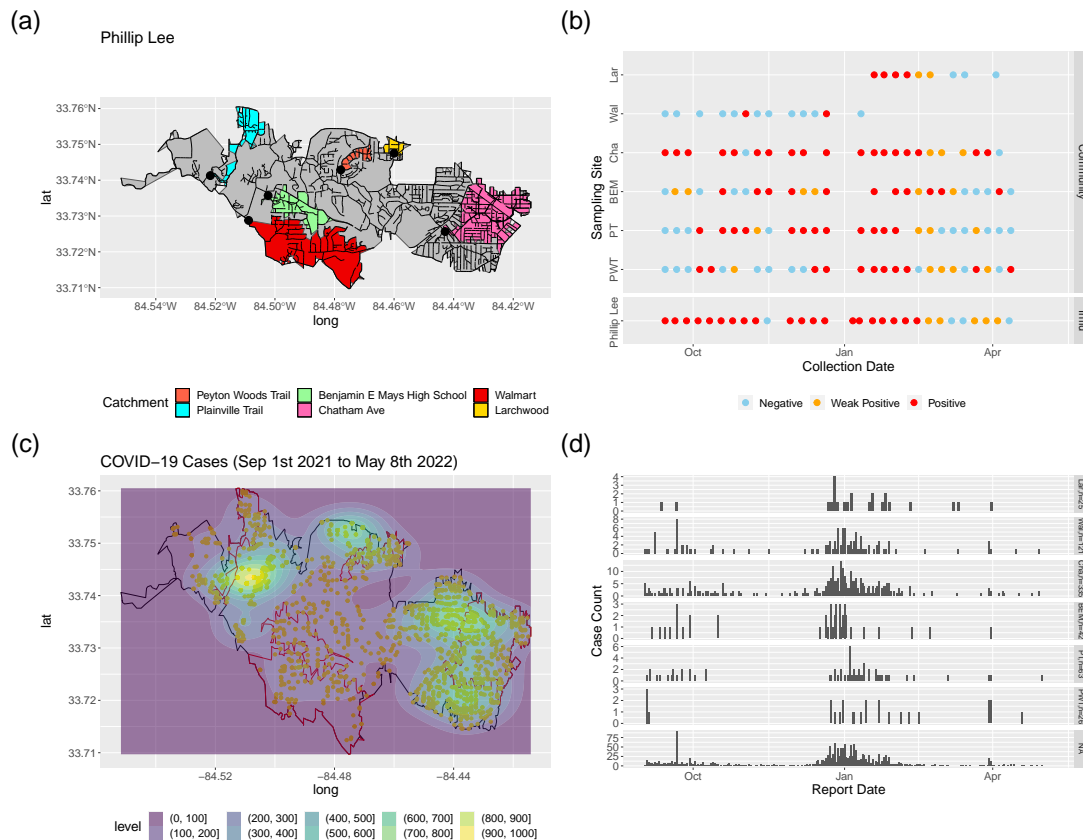


Figure 6: SARS-CoV-2 wastewater surveillance results for community sites and reported COVID-19 case numbers in the catchment area for the Phillip Lee sampling cluster between September 2021–May 2022. Subfigure (a) shows the catchment areas of each community site nested within the overall catchment of the influent line site (in gray). The black lines represent the sewer network lines. Subfigure (b) shows the weekly wastewater surveillance results (RT-PCR detection of SARS-CoV-2 RNA). Subfigure (c) shows the heatmap of reported COVID-19 cases between September 1st 2021–May 8th 2022 within the influent catchment area. Subfigure (d) shows the epidemic curves of COVID-19 within each community site catchment area and NA represents all the cases in the catchment area of the influent line site that are not in the catchment area of a specific community site. PWT, PT, BEM, Cha, Wal, and Lar represent Peyton Woods Trail, Plainville Trail, Benjamin E Mays High School, Chatham Ave, Walmart, and Larchwood respectively.

140 Designing a sensitive and actionable WWS system requires a good understanding of what contributing
 141 population or catchment area is represented in a wastewater sample. With a well-characterized sewerage
 142 system, the catchment area (and population) can be determined for any sampling site within the sewer
 143 network. SARS-CoV-2 RNA concentrations in wastewater collected from such a sampling site reflect

ongoing infections in the population who reside in its catchment area. However, sewerage systems usually develop along with the urbanization process. Combined sewers are common in some historical areas, and sanitary sewers are usually added as a city develops and expands. In the city of Atlanta, combined sewers are mainly located in the city center, which is also the most densely populated area of the sewer network. For WWS, sampling at sites from combined sewers poses challenges to interpretation of the results. First, because the combined sewer collects both sewage and stormwater, the concentration of SARS-CoV-2 RNA in the wastewater can be impacted by extreme variation in flow rate and velocity (caused by rainfall) and any chemicals in the stormwater, which may reduce the sensitivity or inhibit the lab assay. In the city of Atlanta, the Intrenchment, Proctor Creek, and Peachtree Creek influent line sites catch large proportions of combined sewers. Second, areas with combined sewers were observed to have many cross-connections (higher connectivity), which may have been designed to avoid blockage and overflow. Catchment areas and populations can not be precisely determined for sampling sites in such sewer networks.

It is critical that catchments of different sampling sites are discrete areas so that the sources of human excreta entering the catchment can be considered independent. Usually, influent lines are separate and distinct before merging at a wastewater treatment facility. Each line typically represents a large proportion of the city. For community manhole sites, any upstream and downstream connection creates challenges interpreting results regardless of whether they are quantified RNA estimates or presence/absence. For example, when upstream and downstream sites are both positive for SARS-CoV-2, we can not determine whether there are COVID-19 infections located in areas covered by the downstream site but not by the upstream site. Independent catchment areas enable a more straightforward approach for linking WWS results with SARS-CoV-2 infections in specific catchment areas (and populations). The selection of independent locations within the network can be achieved with network partitioning methods [29, 30], and in this study we developed a “*main trunk and branch sites*” method to achieve this goal. Some limitations are introduced by forcing independence between sites. First, it is challenging to identify independent sites in a sewer network with many cross-connections. The sites selected could have extremely large or extremely small catchment areas. Second, in a tree topology sewer network, a small number of branch sampling sites may only be able to cover a proportion of the sewer network. A careful selection of *branch sites* (multiple sites as a system) should be located on a tree topology sanitary sewer network, have independent catchment areas, and together capture wastewater inputs from as large an area of interest as

possible.

At the city level, routine COVID-19 WWS, with weekly or multiple samples per week, could be conducted as a supplemental or alternative method of epidemiological surveillance to provide incidence information for large areas of a city. Although estimating the number of COVID-19 cases or SARS-CoV-2 infections (symptomatic and asymptomatic) directly from wastewater results involves many factors [35], the time course of SARS-CoV-2 RNA level in wastewater should reflect the time course of numbers of viral shedders in the population connected to the sewerage system. Similar to previous studies [36, 37, 38, 39], this study found temporal correlations between SARS-CoV-2 RNA concentrations in wastewater and numbers of daily COVID-19 cases reported. With weekly sample collection, we observed a 7–12 days lead time in wastewater signal trends in influent line samples compared to trends in reported cases in the catchment areas for these influent line sites. This finding demonstrates the potential of WWS to provide early warning of COVID-19 case surges in the city, which could forecast needs for clinical and diagnostic testing resources. However, there was also some discordance between the trends of the SARS-CoV-2 RNA concentration in wastewater and the number of reported COVID-19 cases. Many wastewater samples from the South Fulton influent line were negative for SARS-CoV-2 RNA even when there was a large number of reported cases in the catchment area. We have been exploring the reasons for this finding by measuring pH values, suspended solids, and turbidity of all the wastewater samples from influent lines since July 2021. Higher pH values (>10) were frequently measured (68%) in the wastewater samples collected from the South Fulton influent line compared to pH values (around 7) in the wastewater samples from other influent lines. High pH may denature the virus and degrade the viral RNA, and it may also indicate the presence of other chemicals in wastewater that may cause PCR inhibition. We also observed sustained high SARS-CoV-2 RNA concentrations in some influent line samples after the reported COVID-19 case numbers declined, which could be caused by prolonged fecal shedding [40] or may indicate continuing silent transmission in some communities. The SARS-CoV-2 RNA concentration in wastewater may be considered to represent the number of infected people currently shedding the virus in their feces, rather than COVID-19 incidence. Therefore, concentrations of SARS-CoV-2 RNA in wastewater can be considered a distorted reflection of the reported numbers of COVID-19 cases, convoluted by the fecal shedding curve which causes delay and averages over a certain time period. This distortion weakens the correlation between concentrations of SARS-CoV-2 RNA in wastewater and numbers of COVID-19 cases reported. Silent transmission occurs when an asymp-

204 tomatic case passes the virus to someone else. As the pandemic continues, there will be more people
 205 with some level of immunity, who may be infected with mild or no symptoms. Those infections, which
 206 may be not captured by epidemiological surveillance based on diagnostic testing, are still contributing to
 207 the disease transmission and are shedding SARS-CoV-2 in their feces. In such a scenario, WWS is valu-
 208 able to guide public health response especially in settings where resources are limited or there is severe
 209 underreporting/under-ascertainment.

210 Sampling wastewater from upstream community sites in addition to sampling from downstream influent
 211 sites (i.e., nested sampling) improves the sensitivity of wastewater-based surveillance system. SARS-
 212 CoV-2 RNA signals at downstream sites could be subject to large dilution, rapid degradation of virus and
 213 viral RNA, and substantial loss of signal while moving through the sewer lines [15]. In this study, while
 214 the samples from South Fulton influent line site frequently failed to detect SARS-CoV-2 potentially due
 215 to high pH values, wastewater samples from its upstream community sites consistently tested positive
 216 for SARS-CoV-2 RNA. In this type of situation, sampling only from the downstream influent line site
 217 produced false negative results. And when the disease incidence is low, the concentration of SARS-CoV-
 218 2 RNA could be diluted to a level below the limit of detection whereas sampling at the upstream sites,
 219 that are closer to the shedders, could be more sensitive [15].

220 With an estimated over 413 million people infected with SARS-CoV-2 and 4.27 billion people fully
 221 vaccinated worldwide [41], immunity has gradually increased in the population. However, acceptance and
 222 availability of COVID-19 vaccines are not uniformly distributed [42] resulting in more heterogeneous and
 223 localized COVID-19 transmission [43]. Given these circumstances, more targeted prevention and control
 224 measures are needed to allocate the resources (testing capacity, vaccines, health communications, and
 225 healthcare resources) to those communities at risk. Reported COVID-19 cases can be geocoded with the
 226 assistance of other existing data systems (e.g., voting registration, vehicle registration, medical records
 227 etc.) to identify spatial clustering of cases. However, geocoding all reported cases is not a standard
 228 procedure in the epidemiological surveillance and requires tremendous effort. In this study, we evaluated
 229 the feasibility of using WWS at the community level to trace disease hotspots in a spatial area. With a
 230 nested sampling design, *branch sites* that cover high COVID-19 incidence areas tend to have high SARS-
 231 CoV-2 RNA detection rates. This study demonstrates how such spatial coincidence enables WWS to be
 232 deployed to locate infection clusters.

233 Community level WWS with a small number of independent sampling sites usually cannot cover the

entire geographic area. The adaptive sampling method in the current study allows relocation of sites not detecting SARS-CoV-2 and searching for hotspots in the area. Furthermore, with immunity waxing and waning in the population, and the periodic introduction of new SARS-CoV-2 variants, disease transmission will continue to vary both temporally and spatially. For example, populations in COVID-19 hotspots during the latest Omicron wave (December 2021–February 2022) may gain some level of immunity and be less likely to contribute to SARS-CoV-2 transmission for several months afterwards. Then, the COVID-19 hotspots for the next wave of infection could move to areas where the population has a low level of immunity. An adaptive sampling approach can transform WWS into a dynamic system to identify and trace COVID-19 hotspots in communities.

This study highlights the importance of carefully designed sampling strategies for developing a sensitive and sustainable WWS. We have developed, applied, and validated a novel nested sampling strategy with adaptive sampling process, which enables identification and tracing of COVID-19 hotspots. The strategic sampling design described here is critical for long-term sustainability of WWS for COVID-19 and other diseases, and provides maximum value of information from a minimum number of samples. The spatial granularity of this wastewater surveillance data provides actionable information to guide COVID-19 prevention and control measures at different geographic levels.

Methods

Study Area

The current study was conducted in the city of Atlanta, which is the capital and most populous city (498,715 in 2020) within the state of Georgia. The City of Atlanta Department of Watershed Management (DWM) manages the wastewater system in Atlanta and serves 1.2 million customers within the Atlanta Metropolitan Area. There are three water reclamation centers (WRCs) within the city limits of Atlanta, and each WRC has multiple influent lines (Figure 3a). South River WRC has a permitted treatment capacity of 48 million gallons per day (MGD) and provides wastewater treatment for portions of Atlanta, East Point, Hapeville, College Park, and parts of DeKalb County and Clayton County. Utoy Creek WRC has a permitted treatment capacity of 40 MGD and provides wastewater treatment for portions of Southwest and Northwest Atlanta, East Point, and Fulton County. R.M. Clayton is the largest among the three WRCs, with a permitted treatment capacity of 100 MGD. R.M. Clayton provides wastewater treatment

services for the City of Atlanta, primarily north of Interstate 20, a portion of Sandy Springs, and Northern DeKalb County. Detailed information on the WRCs and the sampled influent lines can be found in Supplementary Table 1. The community sampling sites in this study were selected mainly in the southern part of the city (south of Interstate 20), where underserved neighborhoods (e.g., Adamsville, Oakland City, Pittsburgh, Mechanicsville, and the West End) are located (Figure 3b). The Georgia Department of Community Affairs defined underserved areas as areas with the highest unemployment rate, the lowest per-capita income and the highest percentage of residents whose incomes are below the poverty level. People living in the underserved areas, when infected by SARS-CoV-2, are less likely to seek health care and get tested, leading to higher levels of COVID-19 under-reporting and under-ascertainment via traditional epidemiological surveillance.

Sewer Network and Catchment Identification

Once the SARS-CoV-2 viruses in feces enter sewage, they are transported through the sewerage system consisting of sewers (gravity sewers and force mains), manholes, pumping stations, and wastewater treatment facilities. A sewerage system can be viewed as a flow network with manholes (potential sampling sites) as nodes, sewer segments as edges, and wastewater treatment facilities as sinks which only have incoming flows. The directions of edges represent the flow direction of sewage in sewer lines. If pumping stations are not involved, the sewage flow is only driven by gravity, and the flow direction is determined by the elevation.

A simplified flow network (e.g., rivers, sewerage system) could have a line, tree, or net topology. In a line topology network, the water flows from one upstream point (node) to one downstream point without merging or splitting (Figure 7a). The indegree (the number of edges entering the node) and outdegree (the number edges leaving the node) both equal 1 for all the nodes in the network. A tree topology network has multiple upstream branches (edges) that merge as they flow downstream (Figure 7b). The indegree could be larger than 1 for some nodes while the outdegree equals 1. The larger the average indegree of nodes, the more branches exist within the tree network. In a net topology network, the flow could split and merge multiple times as the water travels downstream (Figure 7c). The indegree and outdegree both are larger than 1. The larger the indegree and outdegree, the higher the connectivity within the network. A sewer network has a hybrid topology integrating line, tree, and net topologies. Usually, sewage is collected from geographically widespread points and moves to the final destination of a wastewater treatment facility. In

291 this type of network, the majority of nodes have outdegrees equal to 1, and the sewer lines (edges) are
 292 merging, developing mainly a tree topology. In this study, we examined the network statistics (indegree
 293 and outdegree) and network topology of the Atlanta sewer network using geospatial data for the Atlanta
 294 sewerage system (with flow direction), in shapefile format, provided by the DWM.

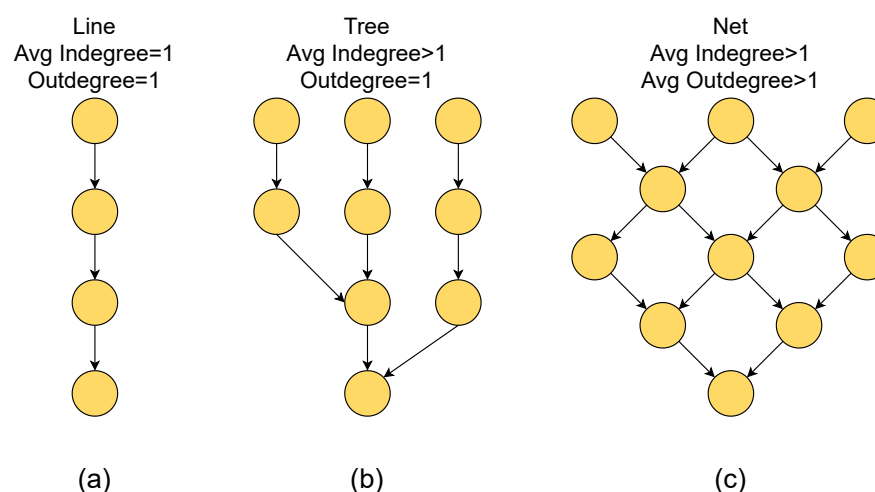


Figure 7: Indegree and outdegree of different flow network topologies.

295 For WWS, it is critical to understand the geographic area and approximately how many people are repre-
 296 sented in each wastewater sample. Based on the sewer network data, we identified all the upstream points
 297 (nodes) and sewer lines (edges) for any potential sampling site (manhole) in the sewer network using
 298 “lucy” [44], a wrapper for the igraph package in R. In the current study, such an upstream sub-network
 299 was defined as the catchment of a sampling point. The catchment area was estimated as the polygon
 300 area covering this sub-network using the “concaveman” package [45] in R, and the catchment size was
 301 approximated by information on the number of upstream manholes (including the sampled manhole).

302 ***Sampling Design and Sample Collection***

303 One of the main purposes of this WWS study was to monitor COVID-19 incidence in the city of Atlanta
 304 at a city level. In this study, the incidence was defined as the number of new COVID-19 cases reported
 305 to the Georgia Department of Public Health (GDPH) over a specific period of time. During March
 306 2021–April 2022, weekly 1 L grab samples of wastewater were collected on Monday mornings at six
 307 influent lines of two water reclamation centers (Utoy Creek and South River), identified by partners at the

DWM. Since November 2022, samples were also collected from three additional influent lines at the R.M. Clayton WRC. The samples from each influent line represent large areas of the city (Figure 3a) and were intended to monitor temporal trends of incidence within each catchment area. To further assess COVID-19 incidence in smaller geographic areas, samples were collected from upstream community sites at manholes. Unlike wastewater from the influent lines, upstream wastewater is less likely to contain SARS-CoV-2 RNA. The Moore swabs method [46], a low-cost composite sampling approach, was used for community site sampling. During April 2021–April 2022, Moore swabs were placed weekly in manholes across the city of Atlanta (Figure 3b) and retrieved after approximately 24 hours. The details of site identification, sampling requirements, sampling schedule, and the mobile data collection process are described in Supplementary Material A.

We developed the Atlanta WWS sampling design for community sites in three phases. In the pilot phase 1 (April–May 2021), information related to the sewer network was not available. We conducted convenience sampling by selecting community sampling sites (manholes) in low-income neighborhoods in South Atlanta based on insights from our partners at DWM. The sampling sites were relocated to new sites every two weeks to explore sampling in different areas of the city and examine the variation in detection rates at different community sites. In phase 2 (June–August 2021), we obtained the Atlanta sewer network shapefile from the DWM, which enabled us to identify the catchment areas and catchment sizes for all manholes. Based on the catchment sizes (measured as number of manholes upstream of the target manhole), we were able to select sampling sites with small, medium, and large catchment sizes (Supplementary Table 2). Three community sites with low detection rates were relocated after four weeks. In phase 3 (September 2021–April 2022), we set up a nested sampling design by sampling one downstream influent line site along with multiple upstream *branch sites* (community manholes), which was defined as a sampling cluster. Using the Phillip Lee sampling cluster as an example (Supplementary Figure 1), we identified the *main trunk*, which was the longest path in the sewer network with the influent line site as the end point. Tributary *branch sites* were defined as the points (nodes) before merging into the *main trunk*. The *branch sites* were independent of each other (no upstream and downstream relationship), and the initial goal was to cover as many manholes as possible. Independence between different *branch sites* is critical to identify sub-areas with high incidence. In phase 3, we also applied the adaptive sampling process [15] to relocate community sites within the nested sampling design in January 2022. Sites that were rarely positive for SARS-CoV-2 RNA were replaced with new *branch sites*, which were proposed

338 following the descending order of their catchment sizes (largest to smallest).

339 ***Adaptive Sampling Process***

340 Usually, the independent upstream sampling sites with small catchment areas could not cover the entire
341 influent line site catchment area that we wanted to monitor. Some high incidence areas, if not covered,
342 could be undetected by WWS. The adaptive sampling process relocated a small proportion of sites period-
343 ically based on the most recent WWS results collected. The adaptive sampling process has the following
344 steps:

345 **Initialization** Assuming we are designing nested sampling on a sewer network and n sampling sites are
346 planned, one sample site will be located at a downstream location of the sewer network (end point
347 of sewer network), and $n - 1$ branching sites (before entering the *main trunk*) will be selected based
348 on their cumulative weight. Each of the manholes (nodes) was given a weight as 1 at initialization.
349 The cumulative weight for each manhole is calculated by adding the weights of all the manholes
350 upstream of the target manhole. The *branch sites* are selected as independent (no upstream and
351 downstream relationship between *branch sites*) sites with the largest cumulative weights.

352 **Weighting** Once the sampling sites have been initialized, wastewater is sampled and tested for a couple
353 of rounds. When the presence of SARS-CoV-2 RNA (positive) is detected in samples from a
354 specific site, the weights of manholes within the catchment of this site increase. The percent
355 that the weight increases depends on the proportion of positive samples. On the other hand, if
356 no positive result is detected in samples from a specific site, the weights of manholes within the
357 catchment of this site decrease.

358 **Updating** After the weights of manholes have been adjusted, the *branch sites* are re-selected following
359 the process same as initialization but based on updated cumulative weights. The weighting and
360 updating steps are repeated periodically, and the WWS can be transformed into a dynamic system
361 that updates itself based on the most recent results.

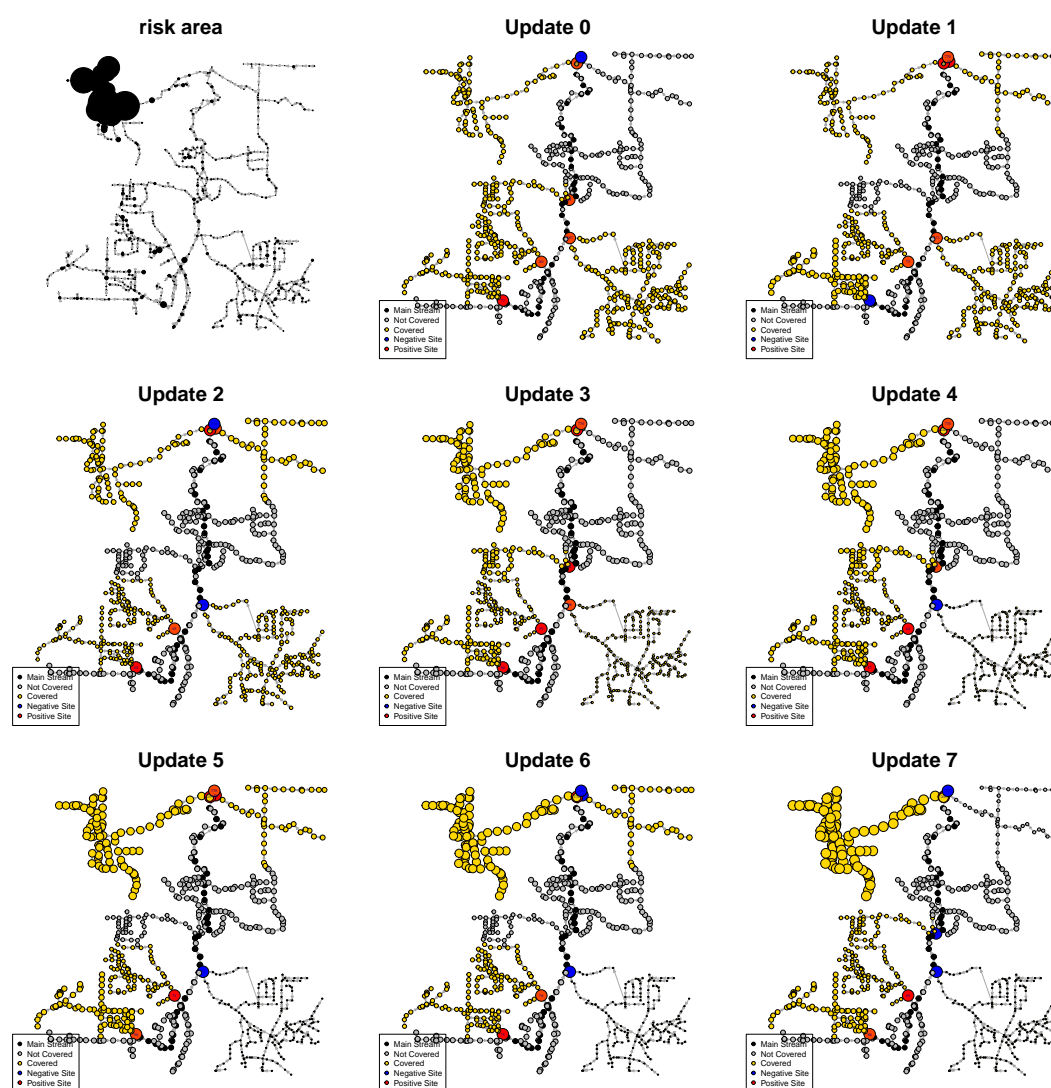


Figure 8: Illustration of adaptive sampling process in a simulation study. Each node is a manhole in the sewer network. Manholes shown in black are on the longest line in the sewer network, defined as the *main trunk* (main stream). Manholes shown in yellow are covered by the selected sampling sites, while manholes shown in gray are not covered. Red manholes represent sites with positive wastewater samples (detection of SARS-CoV-2). Blue manholes represent sites where the wastewater samples were negative. The sizes of nodes represent the weights of sites. The larger the weight, the higher estimated risk of COVID-19 transmission.

362 Figure 8 illustrates the application of the adaptive sampling process in a simulation study. The hypo-
 363 theoretical high-risk area is located at the left top corner of the sewer network. We initialized the sampling
 364 with one site at the end of the sewer network and five branching sites. The weighting and updating steps

were conducted after every two rounds of weekly data collection. As the update process went on, one or two sampling sites were relocated and the weight of the manholes (represented as the size of nodes) on the left top corner increased. The source code of the adaptive sampling process can be found on Github (<https://github.com/YWAN446/COVID-WWS-ATL>).

Sample Processing and Lab Testing

Between March–October 2021, three methods were used to concentrate SARS-CoV-2 from wastewater samples and extract viral RNA: (1) The Membrane Filtration method, which incorporates the use of a 0.45 μm membrane filter, was used to capture SARS-CoV-2 from wastewater grab samples. The Qiagen RNeasy Mini kit (Qiagen, Germany) was used for RNA extraction [46]. (2) The Skim Milk method was used to concentrate SARS-CoV-2 in Moore Swab samples and the same Qiagen RNeasy Mini kit was used as the Membrane Filtration method ([dx.doi.org/10.17504/protocols.io.b2uwqex6](https://doi.org/10.17504/protocols.io.b2uwqex6)). (3) The Manual Nanotrap® Concentration method involved CERES Nanotrap® magnetic hydrogel particles and an enhancement reagent (Ceres Nanosciences Inc., USA). The Nanotrap® Magnetic Virus Particles capture and bind the SARS-CoV-2 viral particles in the wastewater so that they can be concentrated into a smaller volume. The Qiagen QIAamp Viral RNA Mini kit was used for RNA extraction ([dx.doi.org/10.17504/protocols.io.b2uzqex6](https://doi.org/10.17504/protocols.io.b2uzqex6)). The transition between these three methods to our final automated KingFisher Apex system occurred in October 2021 and the MagMax Viral/Pathogen Nucleic Acid Isolation kit (Thermo Fisher Scientific, USA) was incorporated in the KingFisher platform ([dx.doi.org/10.17504/protocols.io.b2nkqdcw](https://doi.org/10.17504/protocols.io.b2nkqdcw)). Each protocol mentioned above utilized a sample processing control of Bovine Respiratory Syncytial Virus (BRSV) (MWI Animal Health, USA), which was spiked directly into wastewater samples prior to sample processing. After concentration and RNA extraction, SARS-CoV-2 and BRSV were detected by a singleplex real-time quantitative reverse transcription polymerase chain reaction (RT-qPCR) ([dx.doi.org/10.17504/protocols.io.b2qyqdxw](https://doi.org/10.17504/protocols.io.b2qyqdxw)) between March–November 2021. After December 2021, a duplex RT-qPCR platform for simultaneous detection of SARS-CoV-2 and BRSV was used between December 2021–April 2022. The details for the RT-qPCR methods were described by Liu et al. [46]. The result was classified as positive when both CT values were present from the duplicate wells and at least one CT value was below 36. If both CT values were present and above 36, the sample was considered as weak positive. When any CT from duplicate wells was absent, the sample was considered negative. For grab samples, the concentrations of SARS-CoV-2

RNA in wastewater were estimated from CT values using standard curves.

Comparing Wastewater Surveillance Results with Reported Case Data

COVID-19 cases reported to the GDPH from March 2021 through April 2022 in Georgia were geocoded using Esri's ArcGIS Streetmap Premium location information for the North America region by GDPH. A set of data sources were used with resident address data from the case report form having the highest priority, followed by electronic laboratory records, and administrative data from other agencies serving Georgia's residents. Coordinates from geocoded resident addresses were used if they passed a series of quality score measures (e.g., resident address matched a single address with the highest score). Records not meeting these quality criteria were excluded. The final data file was the most complete and precise representation of resident address for COVID-19 cases in Georgia.

Wastewater results from any sampling site were matched with a subset of geocoded COVID-19 cases located within the catchment area of the sampling site. For each influent line site, we examined the temporal trends of SARS-CoV-2 RNA concentrations in wastewater and case numbers reported in the catchment area. The concentrations of SARS-CoV-2 RNA were smoothed over time using the LOESS (locally estimated scatterplot smoothing) method. The smoothed concentrations of SARS-CoV-2 RNA and the numbers of daily reported COVID-19 cases in Fulton County/catchment area were analyzed for correlation and temporally lagged correlation. For community sites, we examined the spatial agreement between catchment areas of wastewater sampling sites with high SARS-CoV-2 detection rates and high COVID-19 incidence areas from the geocoded case data. The wastewater detection rate of a site was calculated as the percentage of positive samples and heatmaps of COVID-19 cases were generated using 2D kernel density estimation. Data analysis and data visualization in this study were conducted using R 4.0.1. The maps in Figure 3 were generated by ArcGIS.

The GDPH Institutional Review Board determined that this analysis was exempt from the requirement for IRB review and approval and informed consent was not required.

Data Availability

The dataset of WWS results is available at <https://github.com/YWAN446/COVID-WWS-ATL/data>. The geocoded COVID-19 case data used in this study is available through the Public Health Information Portal

421 data request process (<https://dph.georgia.gov/phil-data-request>).

422 Code Availability

423 The codes for performing the data analyses, data visualization, adaptive sampling process, and simulation
424 study are available at <https://github.com/YWAN446/COVID-WWS-ATL>.

425 References

- 426 1. Peccia J, Zulli A, Brackney DE, et al. Measurement of sars-cov-2 rna in wastewater tracks commu-
427 nity infection dynamics. *Nature biotechnology* 2020;**38**(10):1164–1167. doi:<https://doi.org/10.1038/s41587-020-0684-z>. URL <https://www.nature.com/articles/s41587-020-0684-z>.
428
- 429 2. Izquierdo-Lara R, Elsinga G, Heijnen L, et al. Monitoring sars-cov-2 circulation and diversity
430 through community wastewater sequencing, the netherlands and belgium. *Emerging infectious dis-*
431 *eases* 2021;**27**(5):1405. doi:<https://doi.org/10.3201/eid2705.204410>. URL <https://www.ncbi.nlm.nih.gov/pmc/articles/PMC8084483/>.
432
- 433 3. Kirby AE, Walters MS, Jennings WC, et al. Using wastewater surveillance data to support the
434 covid-19 response—united states, 2020–2021. *Morbidity and Mortality Weekly Report* 2021;
435 **70**(36):1242. doi:<https://doi.org/10.15585/mmwr.mm7036a2>. URL <https://www.ncbi.nlm.nih.gov/pmc/articles/PMC8437053>.
436
- 437 4. Karthikeyan S, Nguyen A, McDonald D, et al. Rapid, large-scale wastewater surveillance and
438 automated reporting system enable early detection of nearly 85% of covid-19 cases on a univer-
439 sity campus. *mSystems* 2021;**6**(4):e00793–21. doi:10.1128/mSystems.00793-21. URL <https://journals.asm.org/doi/abs/10.1128/mSystems.00793-21>.
440
- 441 5. Peixoto VR, Nunes C, Abrantes A. Epidemic surveillance of covid-19: considering uncertainty and
442 under-ascertainment. *Portuguese Journal of Public Health* 2020;**38**(1):23–29. doi:<https://doi.org/10.1159/000507587>.
443
- 444 6. Wang Y, Siesel C, Chen Y, et al. Severe acute respiratory syndrome coronavirus 2 transmission in
445 georgia, usa, february 1–july 13, 2020. *Emerging infectious diseases* 2021;**27**(10):2578. doi:<https://doi.org/10.3201/eid2710.2578>.

- 446 //doi.org/10.3201/eid2710.210061. URL [https://www.ncbi.nlm.nih.gov/pmc/articles/](https://www.ncbi.nlm.nih.gov/pmc/articles/PMC8462336/)
447 [PMC8462336/](https://www.ncbi.nlm.nih.gov/pmc/articles/PMC8462336/).
- 448 7. Ahmed W, Angel N, Edson J, et al. First confirmed detection of sars-cov-2 in untreated wastewater in
449 australia: a proof of concept for the wastewater surveillance of covid-19 in the community. *Science of*
450 *The Total Environment* 2020;**728**:138764. doi:<https://doi.org/10.1016/j.scitotenv.2020.138764>. URL
451 <https://www.sciencedirect.com/science/article/pii/S0048969720322816>.
- 452 8. Medema G, Heijnen L, Elsinga G, Italiaander R, Brouwer A. Presence of sars-coronavirus-2 rna
453 in sewage and correlation with reported covid-19 prevalence in the early stage of the epidemic in
454 the netherlands. *Environmental Science & Technology Letters* 2020;**7**(7):511–516. doi:10.1021/acs.
455 estlett.0c00357. URL <https://doi.org/10.1021/acs.estlett.0c00357>.
- 456 9. Sherchan SP, Shahin S, Ward LM, et al. First detection of sars-cov-2 rna in wastewater in north
457 america: A study in louisiana, usa. *Science of The Total Environment* 2020;**743**:140621. doi:<https://doi.org/10.1016/j.scitotenv.2020.140621>. URL [https://www.sciencedirect.com/science/](https://www.sciencedirect.com/science/article/pii/S0048969720341437)
458 [article/pii/S0048969720341437](https://www.sciencedirect.com/science/article/pii/S0048969720341437).
- 460 10. Chen Y, Chen L, Deng Q, et al. The presence of sars-cov-2 rna in the feces of covid-19 patients.
461 *Journal of Medical Virology* 2020;**92**(7):833–840. doi:<https://doi.org/10.1002/jmv.25825>. URL
462 <https://onlinelibrary.wiley.com/doi/abs/10.1002/jmv.25825>.
- 463 11. Wu Y, Guo C, Tang L, et al. Prolonged presence of sars-cov-2 viral rna in faecal sam-
464 ples. *The Lancet Gastroenterology & Hepatology* 2020;**5**(5):434–435. doi:[https://doi.org/10.1016/](https://doi.org/10.1016/S2468-1253(20)30083-2)
465 [S2468-1253\(20\)30083-2](https://doi.org/10.1016/S2468-1253(20)30083-2). URL [https://www.thelancet.com/journals/langas/article/](https://www.thelancet.com/journals/langas/article/PIIS2468-1253(20)30083-2/fulltext)
466 [PIIS2468-1253\(20\)30083-2/fulltext](https://www.thelancet.com/journals/langas/article/PIIS2468-1253(20)30083-2/fulltext).
- 467 12. Hovi T, Shulman L, Van Der Avoort H, Deshpande J, Roivainen M, De Gourville E. Role
468 of environmental poliovirus surveillance in global polio eradication and beyond. *Epidemiol-*
469 *ogy & Infection* 2012;**140**(1):1–13. doi:<https://doi.org/10.1017/S095026881000316X>. URL
470 [https://www.cambridge.org/core/journals/epidemiology-and-infection/article/](https://www.cambridge.org/core/journals/epidemiology-and-infection/article/role-of-environmental-poliovirus-surveillance-in-global-polio-eradication-and-beyond/DBB1EC7A25FBB252D7EDF9F2F7939FE3)
471 [role-of-environmental-poliovirus-surveillance-in-global-polio-eradication-and-beyond/](https://www.cambridge.org/core/journals/epidemiology-and-infection/article/role-of-environmental-poliovirus-surveillance-in-global-polio-eradication-and-beyond/DBB1EC7A25FBB252D7EDF9F2F7939FE3)
472 [DBB1EC7A25FBB252D7EDF9F2F7939FE3](https://www.cambridge.org/core/journals/epidemiology-and-infection/article/role-of-environmental-poliovirus-surveillance-in-global-polio-eradication-and-beyond/DBB1EC7A25FBB252D7EDF9F2F7939FE3).

- 473 13. Hellmér M, Paxéus N, Magnius L, et al. Detection of pathogenic viruses in sewage provided early
474 warnings of hepatitis a virus and norovirus outbreaks. *Applied and Environmental Microbiology*
475 2014;**80**(21):6771–6781. doi:10.1128/AEM.01981-14. URL <https://journals.asm.org/doi/abs/10.1128/AEM.01981-14>.
476
- 477 14. Andrews JR, Yu AT, Saha S, et al. Environmental surveillance as a tool for identifying high-risk
478 settings for typhoid transmission. *Clinical Infectious Diseases* 2020;**71**(Supplement_2):S71–S78.
479 doi:10.1093/cid/ciaa513. URL <https://doi.org/10.1093/cid/ciaa513>.
- 480 15. Wang Y, Moe CL, Dutta S, et al. Designing a typhoid environmental surveillance study: A simu-
481 lation model for optimum sampling site allocation. *Epidemics* 2020;**31**:100391. doi:<https://doi.org/10.1016/j.epidem.2020.100391>. URL <https://www.sciencedirect.com/science/article/pii/S1755436520300189>.
482
483
- 484 16. Daughton CG. Wastewater surveillance for population-wide covid-19: The present and
485 future. *Science of The Total Environment* 2020;**736**:139631. doi:<https://doi.org/10.1016/j.scitotenv.2020.139631>. URL <https://www.sciencedirect.com/science/article/pii/S004896972033151X>.
486
487
- 488 17. Larsen DA, Wigginton KR. Tracking covid-19 with wastewater. *Nature Biotechnology* 2020;
489 **38**(10):1151–1153. doi:<https://doi.org/10.1038/s41587-020-0690-1>. URL <https://www.nature.com/articles/s41587-020-0690-1>.
490
- 491 18. Covidpoops19 dashboard. URL <https://www.covid19wbec.org/covidpoops19>. Accessed:
492 2022-09-12.
- 493 19. Gonzalez R, Curtis K, Bivins A, et al. Covid-19 surveillance in southeastern virginia us-
494 ing wastewater-based epidemiology. *Water Research* 2020;**186**:116296. doi:<https://doi.org/10.1016/j.watres.2020.116296>. URL <https://www.sciencedirect.com/science/article/pii/S0043135420308320>.
495
496
- 497 20. Wu F, Xiao A, Zhang J, et al. Wastewater surveillance of sars-cov-2 across 40 u.s.
498 states from february to june 2020. *Water Research* 2021;**202**:117400. doi:<https://doi.org/10.1016/j.watres.2021.117400>. URL <https://www.sciencedirect.com/science/article/pii/S0043135421005984>.
499
500

- 501 21. Gibas C, Lambirth K, Mittal N, et al. Implementing building-level sars-cov-2 wastewater surveillance
502 on a university campus. *Science of The Total Environment* 2021;**782**:146749. doi:[https://doi.org/](https://doi.org/10.1016/j.scitotenv.2021.146749)
503 10.1016/j.scitotenv.2021.146749. URL [https://www.sciencedirect.com/science/article/](https://www.sciencedirect.com/science/article/pii/S0048969721018179)
504 pii/S0048969721018179.
- 505 22. Scott LC, Aubee A, Babahaji L, Vigil K, Tims S, Aw TG. Targeted wastewater surveillance of
506 sars-cov-2 on a university campus for covid-19 outbreak detection and mitigation. *Environmental*
507 *Research* 2021;**200**:111374. doi:<https://doi.org/10.1016/j.envres.2021.111374>. URL [https://www.](https://www.sciencedirect.com/science/article/pii/S001393512100668X)
508 [sciencedirect.com/science/article/pii/S001393512100668X](https://www.sciencedirect.com/science/article/pii/S001393512100668X).
- 509 23. Wang Y, Liu P, Zhang H, et al. Early warning of a covid-19 surge on a university campus
510 based on wastewater surveillance for sars-cov-2 at residence halls. *Science of The Total En-*
511 *vironment* 2022;**821**:153291. doi:<https://doi.org/10.1016/j.scitotenv.2022.153291>. URL [https://](https://www.sciencedirect.com/science/article/pii/S0048969722003825)
512 www.sciencedirect.com/science/article/pii/S0048969722003825.
- 513 24. Barrios RE, Lim C, Kelley MS, Li X. Sars-cov-2 concentrations in a wastewater collection sys-
514 tem indicated potential covid-19 hotspots at the zip code level. *Science of The Total Environ-*
515 *ment* 2021;**800**:149480. doi:<https://doi.org/10.1016/j.scitotenv.2021.149480>. URL [https://www.](https://www.sciencedirect.com/science/article/pii/S004896972104554X)
516 [sciencedirect.com/science/article/pii/S004896972104554X](https://www.sciencedirect.com/science/article/pii/S004896972104554X).
- 517 25. Haak L, Delic B, Li L, et al. Spatial and temporal variability and data bias in wastewater surveillance
518 of sars-cov-2 in a sewer system. *Science of The Total Environment* 2022;**805**:150390. doi:<https://doi.org/10.1016/j.scitotenv.2021.150390>. URL [https://www.sciencedirect.com/science/](https://www.sciencedirect.com/science/article/pii/S004896972105467X)
519 [article/pii/S004896972105467X](https://www.sciencedirect.com/science/article/pii/S004896972105467X).
- 520 26. Li J, Ahmed W, Metcalfe S, et al. Monitoring of sars-cov-2 in sewersheds with low covid-19
521 cases using a passive sampling technique. *Water Research* 2022;**218**:118481. doi:[https://doi.org/10.](https://doi.org/10.1016/j.watres.2022.118481)
522 1016/j.watres.2022.118481. URL [https://www.sciencedirect.com/science/article/pii/](https://www.sciencedirect.com/science/article/pii/S0043135422004353)
523 [S0043135422004353](https://www.sciencedirect.com/science/article/pii/S0043135422004353).
- 524 27. Wang JF, Stein A, Gao BB, Ge Y. A review of spatial sampling. *Spatial Statistics* 2012;**2**:1–
525 14. doi:<https://doi.org/10.1016/j.spasta.2012.08.001>. URL [https://www.sciencedirect.com/](https://www.sciencedirect.com/science/article/pii/S2211675312000255)
526 [science/article/pii/S2211675312000255](https://www.sciencedirect.com/science/article/pii/S2211675312000255).
- 527

- 528 28. McCall AK, Palmitessa R, Blumensaat F, Morgenroth E, Ort C. Modeling in-sewer transformations
529 at catchment scale – implications on drug consumption estimates in wastewater-based epidemiology.
530 *Water Research* 2017;**122**:655–668. doi:<https://doi.org/10.1016/j.watres.2017.05.034>. URL <https://www.sciencedirect.com/science/article/pii/S0043135417303986>.
531
- 532 29. Larson RC, Berman O, Nourinejad M. Sampling manholes to home in on sars-cov-2 infections.
533 *PloS one* 2020;**15**(10):e0240007. doi:<https://doi.org/10.1371/journal.pone.0240007>. URL <https://journals.plos.org/plosone/article?id=10.1371/journal.pone.0240007>.
534
- 535 30. Calle E, Martínez D, Brugués-i Pujolràs R, et al. Optimal selection of monitoring sites in cities for
536 sars-cov-2 surveillance in sewage networks. *Environment International* 2021;**157**:106768. doi:<https://doi.org/10.1016/j.envint.2021.106768>. URL [https://www.sciencedirect.com/science/](https://www.sciencedirect.com/science/article/pii/S0160412021003937)
537 [article/pii/S0160412021003937](https://www.sciencedirect.com/science/article/pii/S0160412021003937).
538
- 539 31. Domokos E, Sebestyén V, Somogyi V, et al. Identification of sampling points for the detection of
540 sars-cov-2 in the sewage system. *Sustainable Cities and Society* 2022;**76**:103422. doi:<https://doi.org/10.1016/j.scs.2021.103422>. URL [https://www.sciencedirect.com/science/article/pii/](https://www.sciencedirect.com/science/article/pii/S2210670721006958)
541 [S2210670721006958](https://www.sciencedirect.com/science/article/pii/S2210670721006958).
542
- 543 32. Karim SSA, Karim QA. Omicron sars-cov-2 variant: a new chapter in the covid-19 pandemic. *The*
544 *Lancet* 2021;**398**(10317):2126–2128. doi:[https://doi.org/10.1016/S0140-6736\(21\)02758-6](https://doi.org/10.1016/S0140-6736(21)02758-6). URL
545 [https://www.thelancet.com/article/S0140-6736\(21\)02758-6/fulltext](https://www.thelancet.com/article/S0140-6736(21)02758-6/fulltext).
- 546 33. Michie S, West R, Harvey N. The concept of “fatigue” in tackling covid-19. *BMJ* 2020;**371**. doi:
547 [10.1136/bmj.m4171](https://doi.org/10.1136/bmj.m4171). URL <https://www.bmj.com/content/371/bmj.m4171>.
- 548 34. Petherick A, Goldszmidt R, Andrade EB, et al. A worldwide assessment of changes in adherence to
549 covid-19 protective behaviours and hypothesized pandemic fatigue. *Nature Human Behaviour* 2021;
550 **5**(9):1145–1160. doi:<https://doi.org/10.1038/s41562-021-01181-x>. URL [https://www.nature.](https://www.nature.com/articles/s41562-021-01181-x)
551 [com/articles/s41562-021-01181-x](https://www.nature.com/articles/s41562-021-01181-x).
- 552 35. Wade MJ, Lo Jacomo A, Armenise E, et al. Understanding and managing uncertainty and variability
553 for wastewater monitoring beyond the pandemic: Lessons learned from the united kingdom national
554 covid-19 surveillance programmes. *Journal of Hazardous Materials* 2022;**424**:127456. doi:<https://doi.org/10.1016/j.jhazmat.2022.127456>.

- 555 [//doi.org/10.1016/j.jhazmat.2021.127456](https://doi.org/10.1016/j.jhazmat.2021.127456). URL [https://www.sciencedirect.com/science/](https://www.sciencedirect.com/science/article/pii/S0304389421024249)
556 [article/pii/S0304389421024249](https://www.sciencedirect.com/science/article/pii/S0304389421024249).
- 557 36. Weidhaas J, Aanderud ZT, Roper DK, et al. Correlation of sars-cov-2 rna in wastewater with covid-
558 19 disease burden in sewersheds. *Science of The Total Environment* 2021;**775**:145790. doi:<https://doi.org/10.1016/j.scitotenv.2021.145790>. URL [https://www.sciencedirect.com/science/](https://www.sciencedirect.com/science/article/pii/S0048969721008573)
559 [article/pii/S0048969721008573](https://www.sciencedirect.com/science/article/pii/S0048969721008573).
560
- 561 37. Ai Y, Davis A, Jones D, et al. Wastewater sars-cov-2 monitoring as a community-level covid-19
562 trend tracker and variants in ohio, united states. *Science of The Total Environment* 2021;**801**:149757.
563 doi:<https://doi.org/10.1016/j.scitotenv.2021.149757>. URL [https://www.sciencedirect.com/](https://www.sciencedirect.com/science/article/pii/S0048969721048324)
564 [science/article/pii/S0048969721048324](https://www.sciencedirect.com/science/article/pii/S0048969721048324).
- 565 38. Feng S, Roguet A, McClary-Gutierrez JS, et al. Evaluation of sampling, analysis, and normalization
566 methods for sars-cov-2 concentrations in wastewater to assess covid-19 burdens in wisconsin com-
567 munities. *Acs Es&T Water* 2021;**1**(8):1955–1965. doi:<https://doi.org/10.1021/acsestwater.1c00160>.
568 URL <https://pubs.acs.org/doi/full/10.1021/acsestwater.1c00160>.
- 569 39. Wu F, Xiao A, Zhang J, et al. Sars-cov-2 rna concentrations in wastewater foreshadow dynamics and
570 clinical presentation of new covid-19 cases. *Science of The Total Environment* 2022;**805**:150121.
571 doi:<https://doi.org/10.1016/j.scitotenv.2021.150121>. URL [https://www.sciencedirect.com/](https://www.sciencedirect.com/science/article/pii/S0048969721051962)
572 [science/article/pii/S0048969721051962](https://www.sciencedirect.com/science/article/pii/S0048969721051962).
- 573 40. Zhang Y, Cen M, Hu M, et al. Prevalence and persistent shedding of fecal sars-cov-2 rna in
574 patients with covid-19 infection: A systematic review and meta-analysis. *Clinical and trans-*
575 *lational gastroenterology* 2021;**12**(4). doi:<https://doi.org/10.14309/ctg.0000000000000343>. URL
576 <https://www.ncbi.nlm.nih.gov/pmc/articles/PMC8036078/>.
- 577 41. Our world in data. URL <https://ourworldindata.org/>. Accessed: 2022-02-10.
- 578 42. Hughes MM, Wang A, Grossman MK, et al. County-level covid-19 vaccination coverage and
579 social vulnerability—united states, december 14, 2020–march 1, 2021. *Morbidity and Mortal-*
580 *ity Weekly Report* 2021;**70**(12):431. doi:<https://doi.org/10.15585/mmwr.mm7012e1>. URL <https://www.ncbi.nlm.nih.gov/pmc/articles/PMC7993557/>.
581

- 582 43. Andersen LM, Harden SR, Sugg MM, Runkle JD, Lundquist TE. Analyzing the spatial de-
583 terminants of local covid-19 transmission in the united states. *Science of The Total Environ-*
584 *ment* 2021;**754**:142396. doi:<https://doi.org/10.1016/j.scitotenv.2020.142396>. URL <https://www.sciencedirect.com/science/article/pii/S0048969720359258>.
585
- 586 44. Ness R. lucy. <https://github.com/robertness/lucy>, 2016.
- 587 45. Park JS, Oh SJ. A new concave hull algorithm and concaveness measure for n-dimensional datasets.
588 *Journal of Information science and engineering* 2012;**28**(3):587–600.
- 589 46. Liu P, Ibaraki M, VanTassell J, et al. A sensitive, simple, and low-cost method for covid-19 wastew-
590 ater surveillance at an institutional level. *Science of The Total Environment* 2022;**807**:151047.
591 doi:<https://doi.org/10.1016/j.scitotenv.2021.151047>. URL <https://www.sciencedirect.com/science/article/pii/S0048969721061258>.
592
- 593 47. Atlanta public schools covid-19 case reports. URL [https://www.atlantapublicschools.us/](https://www.atlantapublicschools.us/Page/64958)
594 [Page/64958](https://www.atlantapublicschools.us/Page/64958). Accessed: 2022-02-10.

595 Acknowledgements

596 This project was funded by the NIH Rapid Acceleration of Diagnostics (RADx) initiative with fed-
597 eral funds from the National Institute of Biomedical Imaging and Bioengineering, National Institutes
598 of Health, and the Public Health and Social Services Emergency Fund through the Biomedical Advanced
599 Research and Development Authority, HHS Office of the Assistant Secretary for Preparedness and Re-
600 sponse, Department of Health and Human Services, under Contract No. 75N92021C00012 to Ceres
601 Nanosciences. We thank all the support from Salvins J. Strods and Chipo Chemoyo J. Baker Afame-
602 funa from RADx Initiative, and Dr. Louis J. Vuga from NIH. The data collection was conducted and
603 supported by the City of Atlanta Department of Watershed Management team, including Deputy Com-
604 missioner Quinton Fletcher, Brantley Doctor, Elizabeth Sanchez, Batsirai Nyandebvu, Shatoya Hinkle.
605 We appreciate the discussions with partners at the Georgia Department of Public Health, including Dr.
606 Laura Edison, Dr. Amanda Feldpausch, Cristina Meza, John Olmstead, and Pravara Harati. We appreciate
607 all of the contributions made to this project by colleagues at Ceres Nanosciences, including Ross Dun-
608 lap, Ben Lepene, Dr. Robbie Barbero, and Tara Jones-Roe, who dedicated tremendous effort during the

609 early days of the COVID-19 pandemic to manufacture the Nanotrap Magnetic Virus Particles and rapidly
 610 develop an easy-to-use and powerful set of methods for SARS-CoV-2 RNA concentration from wastew-
 611 ater. This study was also supported by Dr. Allison Chamberlain and Eve Rose from Emory COVID-19
 612 Response Collaborative (ECRC). We thank all the Emory students involved in the study: Stephen Mugal,
 613 Matthew Cavallo, Caleb Cantrell, Jillian Dunbar, Makoto Ibaraki, Kelly Geith, Lindsay Saber, Rebecca
 614 Kann, Keyanna Ralph, Haisu Zhang, Lutf-e-Noor Rahman, and Weiding Fang.

615 **Author Information**

616 ***Contributions***

617 Y.W., P.L., M.W., M.B., P.F.M.T., and C.L.M. conceived study. P.L., J.V., L.G., O.S., L.F., W.R., C.H.,
 618 and M.B. collected data. Y.W., S.P.H., and P.F.M.T. developed the adaptive sampling model and analyzed
 619 data. All authors interpreted results and wrote paper.

620 **Ethics Declarations**

621 ***Competing interests***

622 The authors declare no competing interests.

Supplementary Materials

A Sampling Design and Sample Collection

A.1 Site Identification

Wastewater Treatment Facilities (WWTFs): The City of Atlanta Department of Watershed Management (DWM) routinely collects samples from influent lines of WWTFs for industrial pre-treatment wastewater monitoring. With the consultation of operators at WWTFs, partners at the DWM identified sampling access points for three main influent lines entering each WWTF.

Community Sites: After manholes of community sites were identified using information on the sewer network, the manholes were screened for accessibility in the field. The manholes needed to be accessible and not located in an area with busy traffic (e.g., busy roads) or far from the road (e.g., in the woods). For manholes in grassy or wooded areas, risks were considered for trip hazards (e.g., rocks, sticks, and uneven footing), wildlife (e.g., ticks and snakes), and strenuous hikes. When a manhole was not accessible, the enumerator traced upstream to find an alternative manhole that was accessible.

A.2 Sampling Requirements

Permission: Wastewater sample collection was conducted cooperatively by the Emory University sampling team and the DWM team. The DWM has permission to access and sample from manholes within their jurisdiction (i.e., within the city of Atlanta). For the Emory team to help with the sample collection process, they were required to obtain City of Atlanta contractor badges which were worn in the field. The contractor badges also granted access to the WWTFs without the need for an escort from the DWM team.

Equipment: Depending on the type of samples (grab vs. Moore swab) that were collected, different types of equipment were brought into the field. For collecting grab samples, 1 L autoclavable bottles, metal bucket (with handle) and rope, and long-handled water sample dipper or a painter's pole rigged with a "seat" for the 1 L bottle to sit in were used. For collecting a Moore swab sample, fishing lines (weighted for 50-lb), cotton gauze, bendable metal (e.g., metal coat hanger), a magnetic hook, thin ropes, and a collection bag (e.g., quart-size Ziploc bag, WhirlPak, Biohazard Specimen Transport Bag, etc.) were used. In addition, tape (for labeling collection bottles), a permanent marker, a cooler, ice or ice pack(s), and personal protective equipment (e.g., disposable gowns and gloves, N-95 mask, and face shield etc.)

were used for sample collection as needed. A protocol that describes the materials and methods used in the field to collect Moore swabs and grab samples for wastewater sample collection was published on protocols.io (<http://dx.doi.org/10.17504/protocols.io.b2rzqd76>).

Travel Time: For Atlanta COVID-19 wastewater surveillance, travel time between sites typically ranged from 10 to 30 minutes, cumulatively 1–3 hours of driving per day, which includes the travel time between the laboratory at Emory campus and the sampling sites.

A.3 Sampling Schedule

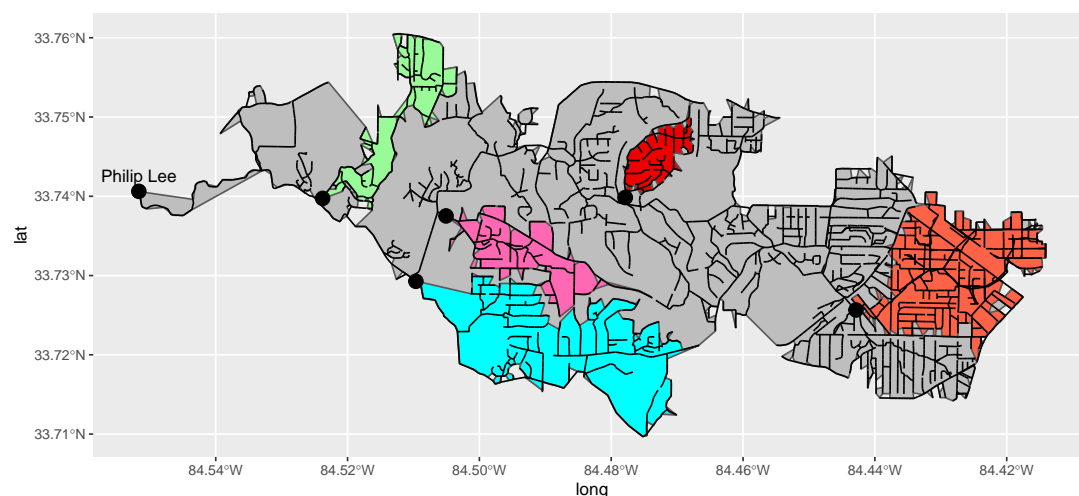
WWTFs: The DWM team collected influent line samples from Utoy Creek Water Reclamation Center and South River Water Reclamation Center. These two plants primarily serve low-income populations in Fulton County. The Emory sampling team collected samples at influent lines of R.M. Clayton plant, which primary serves high-income populations in Fulton County. Grab samples were collected from these nine influent lines every Monday morning, stored in a cooler on ice, and delivered to the laboratory on Emory campus by noon.

Community Sites: The DWM team collected Moore swab samples from manholes located within multiple low-income neighborhoods in South Atlanta. Moore swabs were placed in the wastewater stream of ten manholes on Monday mornings, retrieved on Tuesday mornings, and delivered to the laboratory by 1 PM on Tuesday. Beginning in November 2021, the DWM team began collecting Moore swabs at six additional sites over the weekend (placed on Saturday mornings and retrieved on Sunday mornings). After swabs were retrieved on Sunday, they were stored overnight in a refrigerator at 4 °C, picked up on Monday mornings at 7:30 AM, and delivered to the laboratory by 8:00 AM.

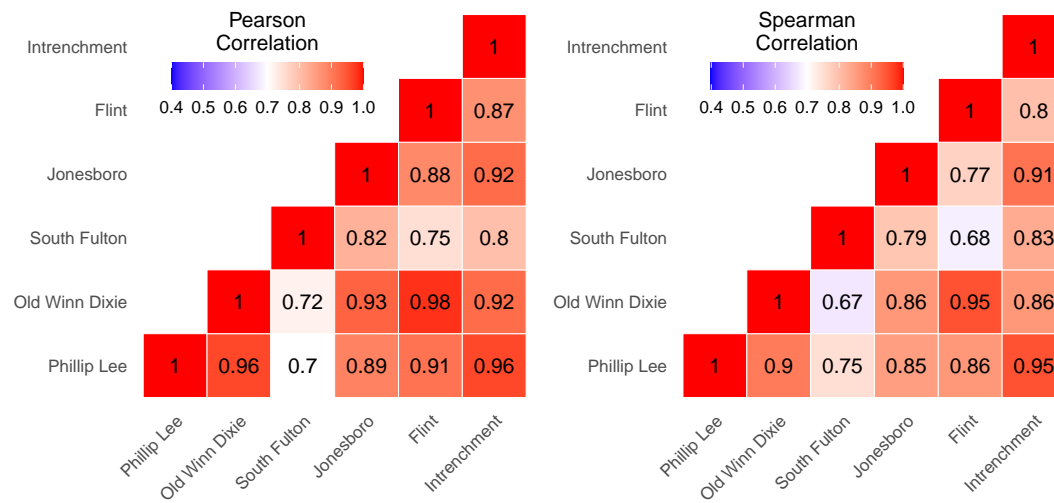
A.4 Mobile Data Collection

The DWM GIS team utilized Esri's Field Operations Apps, including ArcGIS Workforce, ArcGIS Field Map, and ArcGIS Survey123, to conduct the field data collection. ArcGIS Workforce allowed sampling teams to be assigned specific manholes to collect samples from thus avoiding confusion if multiple manholes were present in the area. A dispatcher created weekly sampling assignments from ArcGIS Workforce's web-based map. The sample collection teams used ArcGIS Workforce's mobile app to view assignments, get driving directions, and open ArcGIS Field Maps mobile app. ArcGIS Field Maps allowed teams to view and interact with City of Atlanta's sewerage system. A custom URL was created

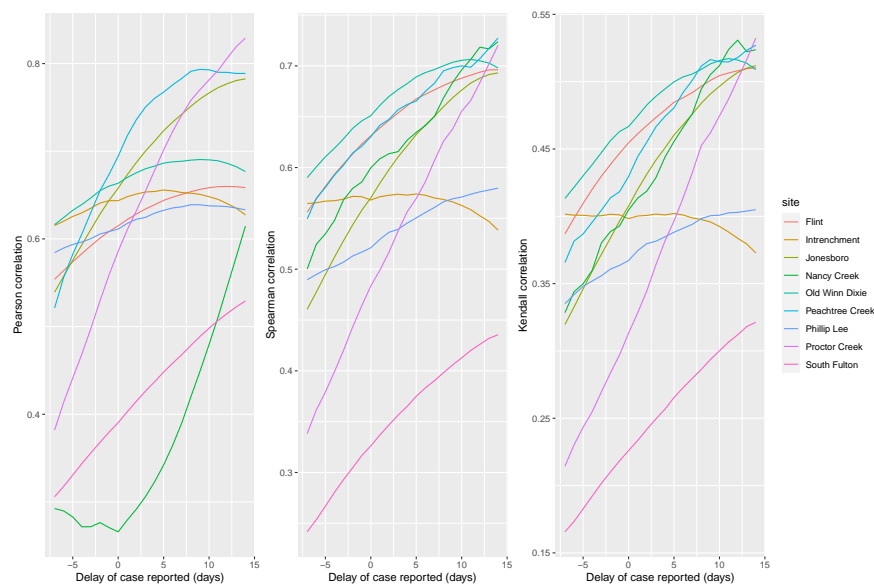
678 and linked to a form in ArcGIS Survey123. The custom URL was configured to communicate attributes
679 of the sampled manhole (e.g., manhole ID, pipe size etc.) to ArcGIS Survey123 and avoid teams having
680 to copy and paste data. Collection date and time, team members ID, and geographic location informa-
681 tion were automatically populated when the form in ArcGIS Survey123 opened. Teams then filled out a
682 few questions, took photos of sampling site, and scanned the barcodes on the bottles or collection bags.
683 The barcode number was then populated in the form. The teams submitted the forms in the field using
684 cellular data and then continued to the next assigned sampling site. Later, the teams entered the date and
685 time the bottles were delivered to the lab at Emory University for testing. ArcGIS Survey123 created a
686 point feature in a feature layer in ArcGIS Online. These feature layers were analyzed in ArcGIS Pro and
687 exported in multiple data formats. Results from the lab were then populated in ArcGIS Online. ArcGIS
688 Dashboards used the feature layer to display the data. Widgets in ArcGIS Dashboards were configured
689 to sort the data by date, council district, and neighborhood planning unit (NPU). The integration between
690 multiple apps and the seamless transfer of data is the reason why Esri Field Operations Apps were chosen.
691 The required training was minimal due to the intuitive work flow of the apps.



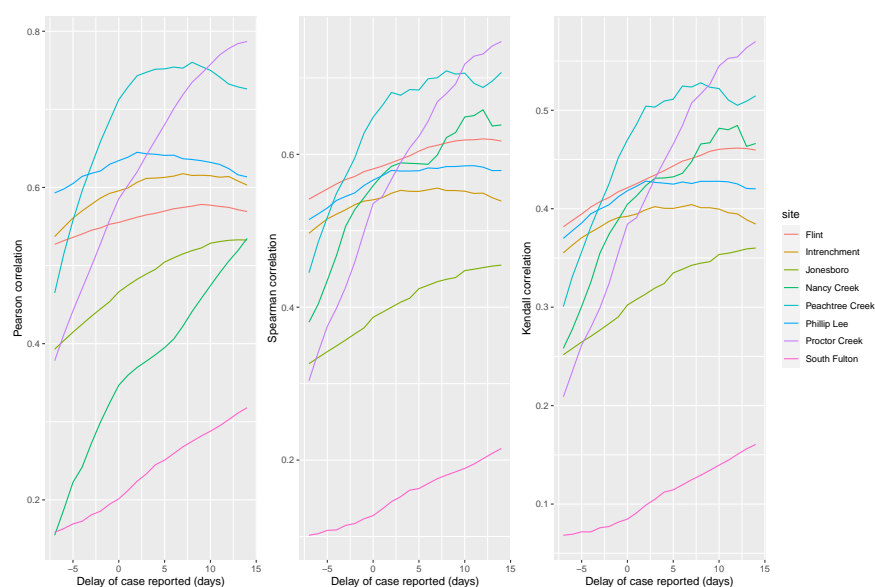
Supplementary Figure 1. Illustration of nested sampling design for the Phillip Lee sampling cluster, including one influent line site and five independent community sites nested within the catchment area of the Phillip Lee influent line site. The gray polygon represents the catchment area of the Phillip Lee influent line site. The five polygons with different colors represent catchment areas of specific community manhole sites.



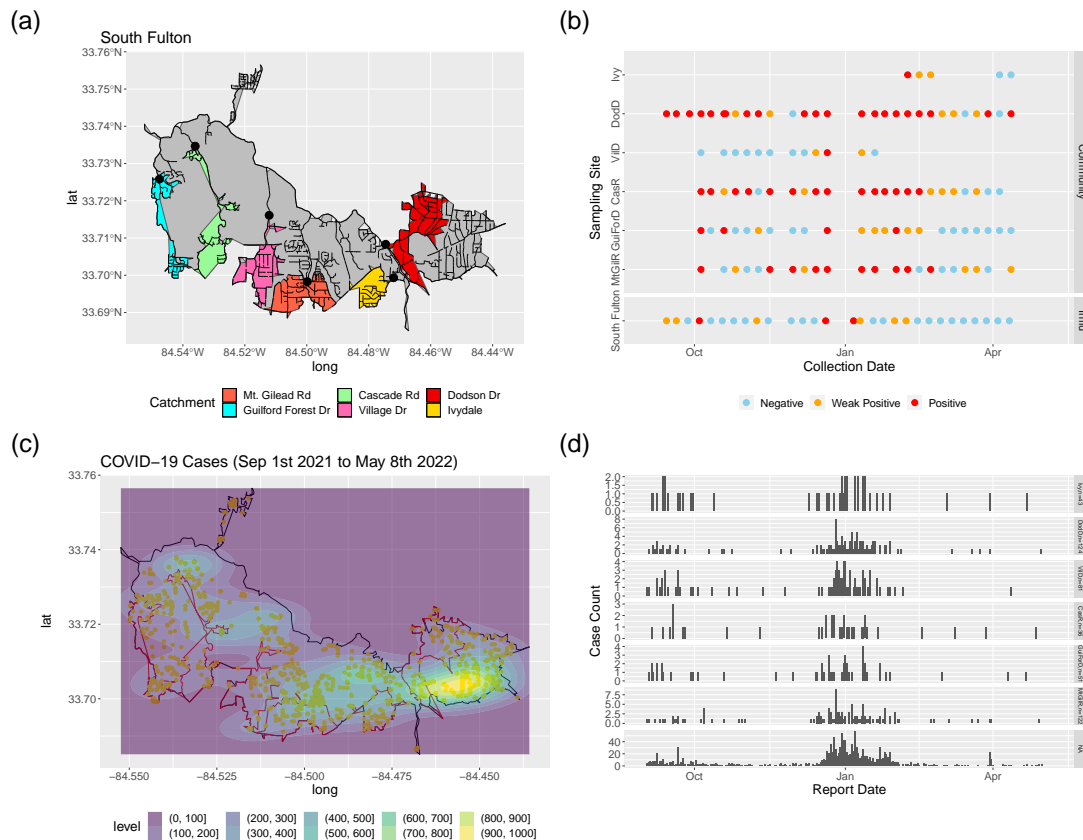
Supplementary Figure 2. Correlations between SARS-CoV-2 RNA concentrations in the wastewater samples from six influent line sites.



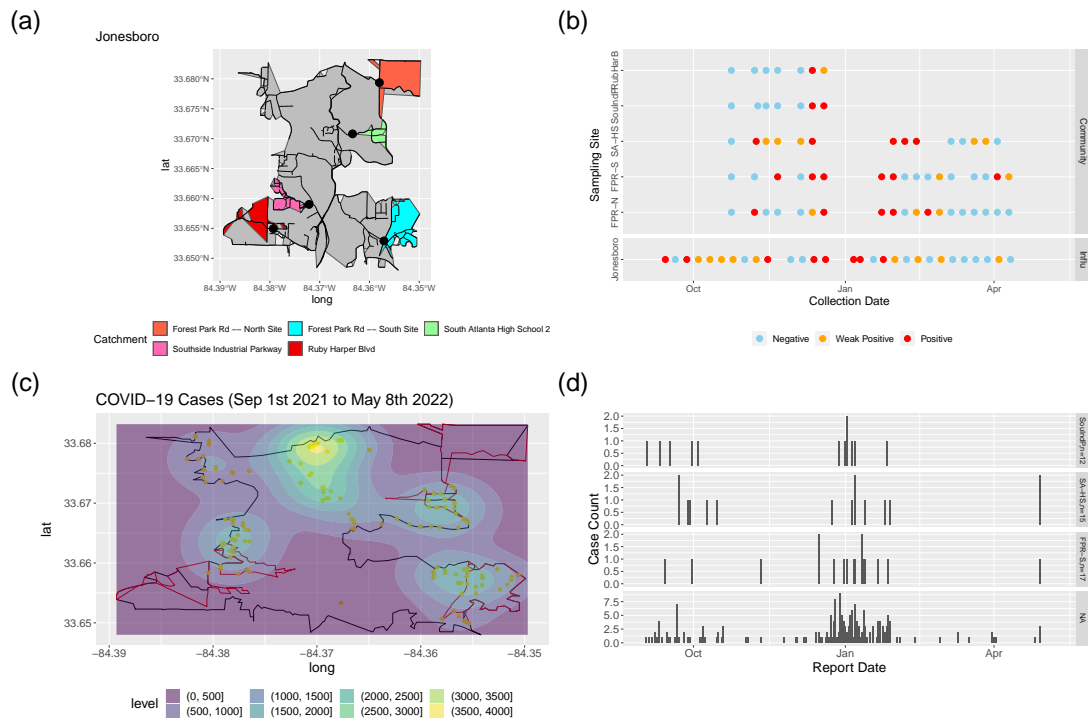
Supplementary Figure 3. Correlations between SARS-CoV-2 RNA concentrations in the wastewater samples and delayed reported case numbers in Fulton County by influent line site.



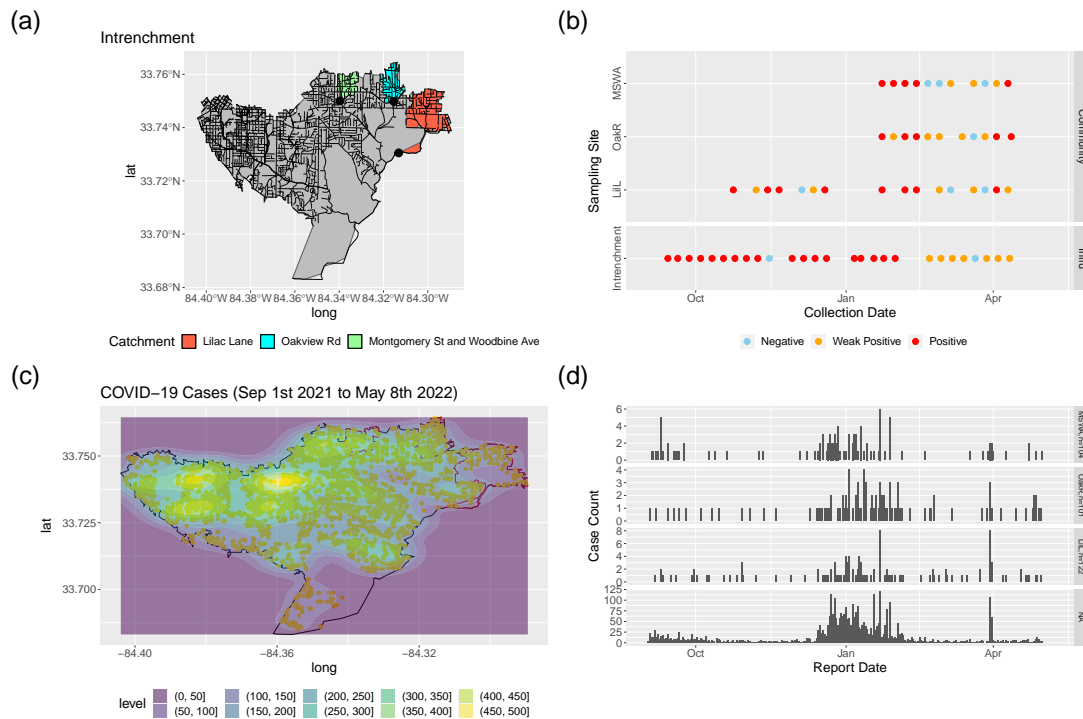
Supplementary Figure 4. Correlations between SARS-CoV-2 RNA concentrations in the wastewater samples and delayed reported case numbers in the influent line catchment area by influent line site.



Supplementary Figure 5. SARS-CoV-2 wastewater surveillance results for community sites and reported COVID-19 case numbers in the catchment area for South Fulton sampling cluster between September 2021–May 2022. Subfigure (a) shows the catchment areas of each community site nested within the overall catchment of the influent line site (in gray). The black lines represent the sewer network lines. Subfigure (b) shows the weekly wastewater surveillance results (RT-PCR detection of SARS-CoV-2 RNA). Subfigure (c) shows the heatmap of reported COVID-19 cases between September 1st 2021–May 8th 2022 within the influent catchment area. Subfigure (d) shows the epidemic curves of COVID-19 within each community site catchment area and NA represents all the cases in the catchment area of the influent line site that are not in the catchment area of a specific community site. MtGILR, GuiForD, CasR, ViLD, DodD, and Ivy represent Mt. Gilead Rd, Guilford Forest Dr, Cascade Rd, Village Dr, Dodson Dr, and Ivydale respectively.



Supplementary Figure 6. SARS-CoV-2 wastewater surveillance results for community sites and reported COVID-19 case numbers in the catchment area for Jonesboro sampling cluster between September 2021–May 2022. Subfigure (a) shows the catchment areas of each community site nested within the overall catchment of the influent line site (in gray). The black lines represent the sewer network lines. Subfigure (b) shows the weekly wastewater surveillance results (RT-PCR detection of SARS-CoV-2 RNA). Subfigure (c) shows the heatmap of reported COVID-19 cases between September 1st 2021–May 8th 2022 within the influent catchment area. Subfigure (d) shows the epidemic curves of COVID-19 within each community site catchment area and NA represents all the cases in the catchment area of the influent line site that are not in the catchment area of a specific community site. FPR-N, FPR-S, SA-HS, SouIndP, and RubHarB represent Forest Park Rd – North Site, Forest Park Rd – South Site, South Atlanta High School, Southside Industrial Parkway, and Ruby Harper Blvd respectively.



Supplementary Figure 7. SARS-CoV-2 wastewater surveillance results for community sites and reported COVID-19 case numbers in the catchment area for Intr trenchment sampling cluster between September 2021–May 2022. Subfigure (a) shows the catchment areas of each community site nested within the overall catchment of the influent line site (in gray). The black lines represent the sewer network lines. Subfigure (b) shows the weekly wastewater surveillance results (RT-PCR detection of SARS-CoV-2 RNA). Subfigure (c) shows the heatmap of reported COVID-19 cases between September 1st 2021–May 8th 2022 within the influent catchment area. Subfigure (d) shows the epidemic curves of COVID-19 within each community site catchment area and NA represents all the cases in the catchment area of the influent line site that are not in the catchment area of a specific community site. LilL, OakR, and MSWA represent Lilac Lane, Oakview Rd, and Montgomery St and Woodbine Ave respectively.

Supplementary Table 1. Descriptive information for influent lines. WRC represents Water Reclamation Center.

WRC	Influent Line	Cover Combined Sewer Area	Cover Industrial Area	# of Manholes Covered	Estimated Catchment Population	ZIP Codes Covered
Utoy Creek	Phillip Lee	No	No	3640	37,552	30311, 30314, 30331, 30310
	Old Winn Dixie	No	No	13	NA	30331
	South Fulton	No	No	2489	39,377	30311, 30331, 30310
South River	Jonesboro	No	Yes	770	5427	30354, 30315
	Flint	No	Yes	2959	29,519	30354, 30315, 30312, 30304, 30303, 30349, 30313, 30310
	Intrenchment Creek	Yes	Yes	7091	79,502	30032, 30315, 30316, 30307, 30312, 30303, 30317, 30313, 30310
R.M. Clayton	Nancy Creek	No	No	3602	41,698	30318, 30319, 30326, 30327, 30305, 30342
	Proctor Creek	Yes	Yes	5923	51,433	30314, 30318, 30303, 30308, 30313, 30310
	Peachtree Creek	Yes	Yes	11,279	178,077	30309, 30318, 30307, 30319, 30312, 30303, 30326, 30327, 30308, 30317, 30306, 30305, 30324, 30342

Supplementary Table 2. Descriptive information for community sites. *The catchment size are calculated as the number of manholes covered.

Name	Type	Manhole ID	Catchment Size*	Associated with Influent Line
1295 West Apartments	Apartment Complex	23150234301	12	Phillip Lee
Cascade Glen Apartments	Apartment Complex	13940319801	1	South Fulton
Columbia Tower at MLK Village	Apartment Complex	23360349501	13	Intrenchment Creek
Country Oaks	Apartment Complex	Unable to identify	NA	Phillip Lee
Fairburn & Gordon II Apartments	Apartment Complex	Unable to identify	NA	NA
Fairway Gardens Apartments	Apartment Complex	Unable to identify	NA	NA
Heritage Station Apartments	Apartment Complex	Unable to identify	NA	NA
Life at Greenbriar Apartments	Apartment Complex	Unable to identify	NA	NA
Pavillion Place Apartments	Apartment Complex	23230107301	50	NA
Peyton Village Apartments	Apartment Complex	Unable to identify	NA	NA
Venetian Hills Apartments	Apartment Complex	23140107401	85	South Fulton
Veranda at Auburn Point	Apartment Complex	23360357501	7	Peachtree Creek
Metropolitan Gardens Condominiums	Apartment Complex	Unable to identify	NA	NA
815 Old Flat Shoals Road	Apartment Complex	23360472211	2	NA
Atlanta Industrial Parkway	Community	13980407601	7494	NA
Benjamin E Mays	Community	13960301201	45	Phillip Lee
Benjamin E Mays High School	Community	13950110501	187	Phillip Lee

Continued on next page

Continued from previous page

Name	Type	Manhole ID	Catchment Size*	Associated with Influent Line
Butler Way NW	Community	23080119001	127	NA
Cambridge Dr & Hogan Rd SW	Community	13930103001	132	NA
Cascade Falls	Community	13950413001	24	Phillip Lee
Cascade Rd	Community	13850100701	235	South Fulton
Chatham Ave	Community	23150132801	733	Phillip Lee
Dodson Dr	Community	23040112201	256	South Fulton
Eloise St SE & Mercer St SE	Community	23350230103	221	Intrenchment Creek
Engelwood Ave SE & Boulevard SE	Community	23350400404	3	Intrenchment Creek
Fair Street SW & Agnes Jones Place	Community	23160442201	105	Proctor Creek
Fairburn Rd	Community	13950100901	221	South Fulton
Forest Park Rd – North Site	Community	23330214201	35	Jonesboro
Forest Park Rd – South Site	Community	23320205701	87	Jonesboro
Guilford Forest Dr	Community	13850103501	222	South Fulton
Ivydale	Community	23040107701	114	South Fulton
Larchwood	Community	23060408001	62	Phillip Lee
Lilac Lane	Community	23550100401	354	Intrenchment Creek
Montgomer St and Woodbine Ave	Community	23460337501	187	Intrenchment Creek
Mt. Gilead Rd	Community	13940200401	259	South Fulton
Oakview Rd	Community	23560310401	217	Intrenchment Creek

Continued on next page

Continued from previous page

Name	Type	Manhole ID	Catchment Size*	Associated with Influent Line
Parsons St SW & Lawshe St SW	Community	23260351103	455	Proctor Creek
Peeples St SW & Cunningham Place	Community	23160455101	108	Proctor Creek
Peyton Woods Trail	Community	23060310701	98	Phillip Lee
Plainville Trail	Community	13860413001	182	Phillip Lee
Pryor St & Richardson St	Community	23260408201	765	Intrenchment Creek
Rockwell St & Coleman St	Community	23250100000	NA	NA
Ruby Harper Blvd	Community	23320107001	44	Jonesboro
Sandy Creek	Community	13970109201	1409	NA
Simon St	Community	23320107101	54	Jonesboro
South Atlanta High School 1	Community	23250320901	1	Flint
South Atlanta High School 2	Community	23330200801	32	Jonesboro
Southside Industrial Parkway	Community	23330305601	60	Jonesboro
Spink St NW	Community	23080102101	60	NA
Victoria Place	Community	23250135301	6	Phillip Lee
Village Dr	Community	13950301801	209	South Fulton
Walmart	Community	13950102901	661	Phillip Lee
Gateway Capitol View	Community	23150422001	1	Flint
Belmonte Hills Townhomes	Community	23150137701	25	Phillip Lee
Cascade Commons	Community	Unable to identify	NA	NA

Continued on next page

Continued from previous page

Name	Type	Manhole ID	Catchment Size*	Associated with Influent Line
Oakland Place Townhomes	Community	23150432601	1	Phillip Lee
Wildwood Townhomes	Community	Unable to identify	NA	NA